

1 **Carbonate saturation state of surface waters in the Ross Sea**  
2 **and Southern Ocean: controls and implications for the onset**  
3 **of aragonite undersaturation**

4  
5 **H. B. DeJong<sup>1</sup>, R. B. Dunbar<sup>1</sup>, D. Mucciarone<sup>1</sup>, D. A. Kowee<sup>1</sup>**

6 [1]{Department of Earth System Science, Stanford University, Stanford, CA, USA}

7 Correspondence to: H. B. DeJong ([hdejong@stanford.edu](mailto:hdejong@stanford.edu))

8  
9 **Abstract**

10 Predicting when surface waters of the Ross Sea and Southern Ocean will become undersaturated  
11 with respect to biogenic carbonate minerals is challenging in part due to the lack of baseline high  
12 resolution carbon system data. Here we present ~ 1700 surface total alkalinity measurements  
13 from the Ross Sea and along a transect between the Ross Sea and southern Chile from the austral  
14 autumn (Feb-Mar 2013). We calculate the saturation state of aragonite ( $\Omega_{Ar}$ ) and calcite ( $\Omega_{Ca}$ )  
15 using measured total alkalinity and  $pCO_2$ . In the Ross Sea and south of the Polar Front,  
16 variability in carbonate saturation state ( $\Omega$ ) is mainly driven by algal photosynthesis. Freshwater  
17 dilution and calcification have minimal influence on  $\Omega$  variability. We estimate an early spring  
18 surface water  $\Omega_{Ar}$  value of ~1.2 for the Ross Sea using a total alkalinity-salinity relationship and  
19 historical  $pCO_2$  measurements. Our results suggest that the Ross Sea is not likely to become  
20 undersaturated with respect to aragonite until the year 2070.

21

22 **1 Introduction**

23 Atmospheric  $CO_2$  concentrations have increased by 40% since preindustrial times to ~400 ppm  
24 today and could ~~double-reach 936 ppm~~ by the year 2100 (IPCC AR5 WG1, 2013). Due to  
25 oceanic uptake of  $CO_2$ , ~~surface ocean pH is already 0.1 units lower than preindustrial values and~~  
26 ~~is the pH of surface waters of the world's oceans are~~ projected to decrease by ~~another~~ 0.3-0.4  
27 units by the end of the century, equivalent to a 50% decrease in carbonate ion ( $CO_3^{2-}$ )

1 concentrations (Orr et al., 2005). Even after CO<sub>2</sub> emissions are halted, it will take thousands of  
2 years before the surface ocean pH returns to ~~the~~ preindustrial levelsstate (Caldeira and Wickett,  
3 2003; Archer et al., 2009).

4 The saturation state ( $\Omega$ ) of seawater with respect to a specific calcium carbonate (CaCO<sub>3</sub>)  
5 mineral (aragonite, calcite, or magnesium calcite) is defined as:

$$6 \quad \Omega = \frac{[Ca^{2+}][CO_3^{2-}]}{K_{sp}} \quad (1)$$

7 where  $K_{sp}$  is the solubility product constant for the specific CaCO<sub>3</sub> mineral and depends on  
8 salinity, temperature, and pressure (Mucci, 1983). Aragonite is ~ 1.6 times more soluble than  
9 calcite at 0°C whereas the solubility of magnesium calcite varies depending on the mole fraction  
10 of magnesium ions (Dickson, 2010).  $\Omega_{Ar}$  represents the saturation state of aragonite and  $\Omega_{Ca}$   
11 represents the saturation state of calcite.  $\Omega < 1$  represents undersaturation where dissolution is  
12 thermodynamically favorable and  $\Omega > 1$  represents supersaturation where precipitation is  
13 favorable. Most surface waters of the global oceans are currently supersaturated with respect to  
14 CaCO<sub>3</sub> (Feely et al., 2009). However, for some species including coccolithophorids,  
15 foraminifera, and tropical corals, decreasing CO<sub>3</sub><sup>2-</sup> concentrations can decrease calcification rates  
16 even in supersaturated conditions (e.g., Riebesell et al., 2000; Moy et al, 2009; Andersson et al.,  
17 2011).

18 The Southern Ocean is especially vulnerable to Ocean Acidification (OA) due to its relatively  
19 low total alkalinity (TA) and because of increased CO<sub>2</sub> solubility in cold water. In addition,  
20 Antarctic continental shelves have insignificant sedimentary CaCO<sub>3</sub> to buffer against OA (Hauck  
21 et al., 2013). Modeling studies predict that sSurface waters in the Southern Ocean may start to  
22 become undersaturated with respect to aragonite by 2050 and be fully undersaturated by 2100  
23 (Orr et al., 2005; Feely et al., 2009). McNeil and Matear (2008) have suggested that wintertime  
24 aragonite undersaturation in the Southern Ocean may begin as early as 2030.

25 OA induced decreases in  $\Omega$  have potentially serious consequences for Antarctic food webs. In  
26 the Ross Sea the aragonitic shelled pteropod *Limacina helicina* is a dominant zooplankton that  
27 can reach densities of 300 individuals m<sup>-3</sup> (Hopkins, 1987; Seibel and Dierssen, 2003; Hunt et  
28 al., 2008). Pteropods are important prey for nototheniid fish, which in turn are major prey for  
29 penguins, seals, and whales (Foster and Montgomery, 1992; La Mesa et al., 2000; 2004).

1 Pteropods may also be important contributors to the biological pump (Collier et al., 2000;  
2 Accornero et al., 2003; Manno et al., ~~2009~~2010). ~~A study by~~ Orr et al. (2005) found that the shell  
3 of a subarctic pteropod started to dissolve ~~after~~ within 48 h when placed in waters with the level  
4 of aragonite saturation expected to occur in the Southern Ocean by 2100. Severe dissolution  
5 pitting was observed on live pteropods that were collected from the upper 200 meters in the  
6 Atlantic sector of the Southern Ocean, from waters that were near undersaturation with respect  
7 to aragonite (Bednaršek et al., 2012).

8 Other organisms in the Southern Ocean may be negatively impacted by OA include krill  
9 (Kawaguchi et al., 2013), foraminifera (Moy et al., 2009), sea urchins (Sewell and Hofmann,  
10 2011), deep sea hydrocorals (Shadwick et al., 2014), ~~coralline algae~~, sea-stars (Gonzalez-Bernat  
11 et al., 2013), bivalves (Cummins et al., 2011), and brittle stars (McClintock et al., 2011).  
12 Conversely non-calcareous phytoplankton may benefit in the Ross Sea in a high pCO<sub>2</sub> world,  
13 especially the larger diatom *Chaetoceros lineola* (Tortell et al., 2008; Feng et al., 2009).

14 There are only a few surface carbon system data sets from the Ross Sea (Bates et al., 1998;  
15 Sweeney et al., 2000b; Sandrini et al., 2007; Long et al., 2011; Mattsdotter Björk et al., 2014;  
16 Rivaro et al., 2014; Kapsenberg et al., 2015) that can be used to establish baselines in order to  
17 understand the relative importance of ~~the~~ physical, chemical, and biological processes that drive  
18 the large spatial and seasonal variability of  $\Omega$ . With no winter  $\Omega$  measurements, it is challenging  
19 to predict when the Ross Sea will become undersaturated with respect to aragonite and calcite. A  
20 model by McNeil et al. (2010) suggests that winter surface waters in the Ross Sea will become  
21 undersaturated with respect to aragonite by the year 2045 since sea ice, upwelling of deep water,  
22 and short residence times prevent these surface waters from reaching equilibrium with the  
23 atmosphere. However, McNeil et al. (2010) indirectly estimated surface winter  $\Omega_{Ar}$  values by  
24 using limited carbon system data from the spring (Sweeney et al., 2000b).

25 We present ~1700 underway TA measurements from the surface waters of the Ross Sea and  
26 along a transect across the Southern Ocean from the Ross Sea to southern Chile. By combining  
27 the underway TA measurements with pCO<sub>2</sub> data we characterize the complete carbon system and  
28 describe patterns and controls on  $\Omega$  variability. Finally, after establishing a relationship between  
29 salinity and TA, we use the Lamont Doherty Earth Observatory (LDEO) pCO<sub>2</sub> database

1 (Takahashi et al., 2009) (available at <http://www.ldeo.columbia.edu/res/pi/CO2>) to provide an  
2 independent estimate of Ross Sea surface water  $\Omega_{Ar}$  in early spring.

3

## 4 **2 Study site**

5 The Antarctic Circumpolar Current (ACC) flows from east to west around the entire Antarctic  
6 continent and is composed of multiple fronts that separate distinct water masses (Rintoul et al.,  
7 2001). There are three primary fronts—the southern ACC front (SACCF), the Antarctic Polar  
8 Front (PF) and the Subantarctic Front (SAF) (Orsi et al., 1995). Sokolov and Rintoul (2009)  
9 found that these primary fronts are composed of multiple jets that they label south (S), middle  
10 (M), and north (N). Convergent Ekman transport north of the westerly wind stress maximum  
11 (near the axis of the ACC) downwells surface water into the ocean interior. Circumpolar Deep  
12 Water (CDW) upwells south of the wind stress maximum where it becomes modified into  
13 Antarctic surface water (AASW) (Rintoul et al., 2001).

14 The cyclonic Ross Sea gyre is located south of the ACC (Smith et al., 2012). The southern  
15 portion of this gyre flows west along the Ross Sea continental slope and generates intrusions of  
16 CDW onto the Ross Shelf through the major troughs (Orsi et al., 2009; Dinniman et al., 2011;  
17 Kohut et al., 2013). In addition, AASW enters the Ross Sea in the east and flows westward along  
18 the Ross Ice Shelf (Orsi et al., 2009).

19 The Ross Sea is considered a biological hotspot supporting over 400 benthic species (Smith et  
20 al., 2012). During the winter the Ross Sea is mostly covered by sea ice, which begins to clear in  
21 November to form the largest polynya in Antarctica. There are two main phytoplankton blooms  
22 in the Ross Sea. The first bloom begins in late November in the Ross Sea polynya (Fig. 1a) and  
23 peaks in mid to late December (Arrigo et al., 1999, 2004). In early January, sea ice melts in the  
24 western Ross Sea lowering surface salinity and increasing stratification (Fig. 1b). As a result, a  
25 secondary diatom bloom forms in the west with productivity peaking in late January to early  
26 February (Arrigo et al., 1999, 2004) (Fig. 1c).

27 ~~As summer approaches, the~~ The Ross Sea supports one of the most productive phytoplankton  
28 blooms ~~in Antarctica, accounting account~~ for up to half of all primary production over the  
29 Antarctic continental shelf (Arrigo and McClain, 1994; Smith and Gordon, 1997; Arrigo and van

Formatted: Font: 12 pt

1 Dijken, 2003). Photosynthesis reduces the concentration of nutrients and dissolved inorganic  
2 carbon (DIC) in the mixed layer, causing  $\Omega$  to increase in surface waters (McNeil et al., 2010).  
3 Once the sea ice reforms during autumn and winter, remineralization of organic matter and deep  
4 convective mixing produces a relatively homogeneous water column, causing surface DIC  
5 concentrations to increase and  $\Omega$  to decrease (Gordon et al., 2000; Sweeney et al., 2000b; Petty  
6 et al., 2013).

7 ~~The Southern Ocean is composed of multiple fronts that separate distinct water masses (Rintoul  
8 et al., 2001). The most prominent are the Antarctic Polar Front (PF) and the Sub-Antarctic Front  
9 (SAF). Circumpolar Deep Water (CDW) upwells south of the PF where it becomes modified into  
10 Antarctic surface water (AASW). We define the fronts based on the sea surface temperature  
11 (SST) gradient after averaging the underway SST data into 0.25° bins. Following Dong et al.  
12 (2006), the PF is defined as the southernmost location at which the SST gradient exceeds  $1.5 \times$   
13  $10^{-2} \text{ } ^\circ\text{C km}^{-1}$ . Following Burling (1961), the SAF is defined as the maximum SST gradient in the  
14 SST range of 5–9°C. During our cruise the PF was located at 65.5°S and the SAF was at 57°S.~~

Formatted: Normal, Indent: Left: 0"

### 16 **3 Methods**

#### 17 **3.1 Carbon system measurements Analytical methods**

18 As part of the TRacing the fate of Algal Carbon Export (TRACERS) program, we ~~made~~  
19 undertook continuous measurements of surface water TA in the western Ross Sea aboard the  
20 *Nathaniel B Palmer* (NBP13-02) from 13 Feb through 9 March 2013. In addition, from 19 Mar  
21 to 2 Apr 2013, we made continuous measurements of surface water TA in transit between the  
22 Ross Sea and southern Chile along the cruise track shown in Fig. 24.

23 Underway TA measurements were conducted using the shipboard uncontaminated continuous  
24 flow system with an intake located at ~ 5 m depth. Seawater from the ship's underway system  
25 was redirected to the bottom of a 250 mL free surface interface cup flowing at 2 L/min and was  
26 drawn from the bottom of the cup for TA analysis without filtration. The entire system was  
27 automated and relatively unattended. The sampling cycle was every 24 minutes on a custom-  
28 configured Metrohm 905 Titrando equipped with three Metrohm 800 Dosino syringe pumps (two  
29 50 mL units for sample handling and rinsing and one 5 mL unit for acid titration). Temperature

1 was measured at the cup and in the titration cell. We used certified 0.1N HCl provided by A.  
2 Dickson (Scripps Institution of Oceanography) for the potentiometric titrations and TA  
3 calculations follow Dickson et al. (2003). Since we consumed the certified HCl after ~ 1000  
4 measurements in the Ross Sea, ~~we have no TA data from the eastern Ross Sea-. For the transect~~  
5 ~~to southern Chile.~~ we mixed our own 0.1N HCl solution ~~for the transect to southern Chile~~ (from  
6 12.1 N HCl, laboratory grade NaCl, and deionized water). We calibrated TA measurements  
7 using certified reference materials (CRMs) Batch 122 provided by A. Dickson (Scripps  
8 Institution of Oceanography). Our estimated precision for the underway TA measurements from  
9 68 CRM analyses is  $\pm 3 \mu\text{mol kg}^{-1}$  ( $\pm 1$  SD).

10 Outlier TA analyses were identified by taking a running mean and standard deviation of 9  
11 consecutive measurements. A measurement was rejected if (1) the difference between the  
12 measurement and mean was greater than twice the standard deviation and (2) the difference  
13 between the measurement and mean was greater than  $6 \mu\text{mol kg}^{-1}$ . A total of 65 measurements  
14 (out of 1716) were rejected.

15 ~~We collected seawater samples for particulate organic carbon (POC) every 2 h from the ship's~~  
16 ~~continuous flow system between the Ross Sea and Chile. Following the protocols of Knap et al.~~  
17 ~~(1996), we filtered 1 to 3 L of seawater through precombusted Whatman GFC filters and~~  
18 ~~immediately rinsed these filters with 10 mL of 0.01N HCl to remove carbonate. We air dried the~~  
19 ~~filters before sending them to Stanford University where they were analyzed on a Carlo Erba~~  
20 ~~NA1500 Series 2 elemental analyzer.~~

21 Surface  $\text{pCO}_2$  measurements were made every 3 minutes using the LDEO air-sea equilibrator  
22 permanently installed on the NBP (data available at <http://www.ldeo.columbia.edu/res/pi/CO2>).  
23 The estimated precision is  $\pm 1.5 \mu\text{atm}$ .

24 ~~Underway salinity and sea surface temperature (SST) were measured continuously by the ship's~~  
25 ~~thermosalinograph (TSG) (Sea-Bird Model SBE-45). These variables were binned into 1 minute~~  
26 ~~intervals.~~

27  
28 ~~In order to evaluate the controls of seasonal surface  $\Omega_{\text{Ar}}$  variability in the Ross Sea, we We~~  
29 ~~collected made~~ discrete water ~~samples~~ ~~column~~ TA and DIC measurements at 85 stations ~~in the~~

**Formatted:** Add space between paragraphs of the same style, Tab stops: 5.14", Left

**Formatted:** Pattern: Clear

**Formatted:** Add space between paragraphs of the same style, Tab stops: 5.14", Left

**Formatted:** English (United States)

**Formatted:** Tab stops: 5.14", Left

1 ~~Ross Sea using Niskin bottles attached to a 24 bottle rosette~~ from 13 Feb through 18 Mar 2013  
2 (Fig. 1a). ~~We used a rosette sampler fitted with 24 Niskin bottles and a Sea-Bird Model SBE-~~  
3 ~~911+ conductivity, temperature, and depth (CTD) sensor. We also measured salinity on discrete~~  
4 ~~underway and hydrocast samples at 25°C using a Guildline 8400 Autosal four-electrode~~  
5 ~~salinometer. The difference between the Autosal measurements and salinity from the~~  
6 ~~conductivity sensor was less than 0.02. In this paper we use the hydrocast samples to evaluate the~~  
7 ~~controls of seasonal surface  $\Omega_{Ar}$  variability. The water column data will be further analyzed in~~  
8 ~~upcoming papers.~~

9 We collected hydrocast samples for TA and DIC following the protocols of Dickson et al. (2007)  
10 and immediately added saturated mercuric chloride (< 0.1% by volume). For TA, we ran each  
11 sample within 12 h of collection using a second potentiometric titrator, a Metrohm 855 Robotic  
12 Titrosampler equipped with two 800 Metrohm Dosino syringe pumps (one 50 mL unit for rinsing  
13 and sample handling and one 5 mL unit for acid titration). The samples were prefiltered through  
14 0.45 $\mu$ m polyvinylidene fluoride filters and the estimated precision based on the CRMs (n=108)  
15 is  $\pm 1.5 \mu\text{mol kg}^{-1}$ .

16 We measured DIC on hydrocast samples within  $\sim 4$  h of collection without filtration. We  
17 acidified 1.25 mL of the sample using a custom built injection system coupled to an infrared gas  
18 analyzer (LI-COR LI7000). As described by Long et al. (2011), the infrared absorption signal  
19 versus time is integrated for each stripped gas sample to yield a total mass of CO<sub>2</sub>. Samples were  
20 run in triplicate or greater and were calibrated using CRMs between every 3-4 unknowns. Micro-  
21 bubbles regularly appeared within injected samples due to sample warming between acquisition  
22 and DIC analysis. Each integration curve was visually inspected and integration curves that  
23 exhibited evidence for bubbles were rejected. The estimated precision based upon unknowns  
24 (>3500 runs) and CRM replicates (n=855) for cruise NPB-1302 is  $\pm 3 \mu\text{mol kg}^{-1}$ .

### 26 **3.2 Carbon system calculations and crosschecks**

27 We calculate  $\Omega$  and DIC (hereafter called DIC<sub>calc</sub>) for underway samples with CO2SYS -for  
28 MATLAB (Lewis and Wallace, 1998; van Heuven et al., 2009) with TA, pCO<sub>2</sub>, SST, and  
29 salinity as input variables. Calculations are only conducted for pCO<sub>2</sub> measured within 3 minutes  
30 of the TA measurement (n=1034), the average cycle time for the automated pCO<sub>2</sub> measurements.

1 We use the equilibrium constants of Mehrback et al. (1973) as refit by Dickson and Millero  
2 (1987) since previous studies have found that they are the optimal choice, including for Antarctic  
3 waters (e.g. ~~McNeil et al., 2007~~, Lee et al., 2000; Millero et al., 2002; [McNeil et al., 2007](#)). For  
4 the hydrocast data, we calculate  $\Omega$  using TA, DIC, temperature, and salinity as input variables.

5 As a means of internal quality control, we use the initial pH reading from the TA titration as a  
6 third carbon system parameter to crosscheck the accuracy of our  $\Omega_{Ar}$  estimates. ~~In terms of~~  
7 ~~consistency~~,  $\Omega_{Ar}$  calculated using TA and  $pCO_2$  is  $0.02 \pm 0.07$  greater than  $\Omega_{Ar}$  calculated using  
8 TA and pH. In addition,  $DIC_{calc}$  using TA and  $pCO_2$  is  $2 \pm 7 \mu mol kg^{-1}$  lower than  $DIC_{calc}$  using  
9 TA and pH. Finally, measured  $pCO_2$  is  $4 \pm 14 \mu atm$  lower than  $pCO_2$  calculated from TA and  
10 pH. These strong consistencies suggest that our  $pCO_2$  and TA measurements are accurate. Our  
11 surface TA and  $DIC_{calc}$  measurements versus latitude for the Southern Ocean are within the  
12 ranges of other studies (~~Mattsdotter Björk et al., 2014~~, ~~McNeil et al., 2007~~, Metzl et al., 2006;  
13 [McNeil et al., 2007](#); [Mattsdotter Björk et al., 2014](#)).

14 We compare the TA measurements from the surface hydrocasts (< 5 meters deep) to the  
15 underway TA measurements made while the ship was still on station within ~ 15 minutes of  
16 when the surface samples were collected. The underway values are  $3 \pm 5 \mu mol kg^{-1}$  higher than  
17 the hydrocast TA values.

18

### 19 **3.3 Ross Sea and Southern Ocean Calculations**

20 The  $\Omega_{Ar}$  of surface waters in the Ross Sea increases during the austral summer months (McNeil  
21 et al., 2010). We use DIC, TA, SST, and salinity to determine the controls on the seasonal cycle  
22 of surface water  $\Omega_{Ar}$ . We normalize DIC and TA to a salinity of 34.5, the average salinity of the  
23 Ross Sea (hereafter called sDIC and sTA). Due to the deep convective mixing during the winter,  
24 we use the average sDIC and sTA concentrations of hydrocast samples collected from 200-400  
25 m to determine winter water values (sDIC =  $2221 \pm 5 \mu mol kg^{-1}$ , sTA =  $2338 \pm 3 \mu mol kg^{-1}$ ).  
26 While sDIC and sTA concentrations below 200 m are influenced by carbon export particularly in  
27 the summer and early autumn, observations show that sDIC and sTA concentrations are  
28 relatively uniform below 200 m across space and a given season (Table 1).



1 Following Hauri et al. (2013), the change in  $\Omega_{Ar}$  of surface hydrocast samples (upper 10 m) from  
2 winter conditions can be expressed as:

$$3 \Delta\Omega_{Ar} = \frac{\partial\Omega}{\partial DIC} \Delta sDIC + \frac{\partial\Omega}{\partial TA} \Delta sTA + \frac{\partial\Omega}{\partial T} \Delta T + \Delta S_{\Omega} + Residuals \quad (2)$$

4 where

$$5 \Delta S_{\Omega} = \frac{\partial\Omega}{\partial S} \Delta S + \frac{\partial\Omega}{\partial DIC} \Delta DIC^s + \frac{\partial\Omega}{\partial TA} \Delta TA^s \quad (3)$$

6  $\Delta sDIC$  and  $\Delta sTA$  are the difference in sDIC and sTA for each sample from the winter value. The  
7 term  $\Delta T$  is calculated using a winter SST of  $-1.89^{\circ}\text{C}$  (per Sweeney, 2003).  $\Delta S_{\Omega}$  represents the  
8 total contribution of salinity changes to  $\Delta\Omega_{Ar}$ .

9 Since salinity between 200 to 400 m is variable across the Ross Sea (Orsi and Wiederwohl,  
10 2009),  $\Delta S$  is calculated as the difference between the salinity of a surface sample and the average  
11 salinity for samples from that station that are between 200-400 m.

12  $\Delta DIC^s$  and  $\Delta TA^s$  represent changes to DIC and TA due to dilution/concentration from freshwater  
13 input and sea-ice processes:

$$14 \Delta DIC^s = [DIC_{200-400} * (Salinity_{surface\ sample}/Salinity_{200-400})] - DIC_{200-400} \quad (4)$$

$$15 \Delta TA^s = [TA_{200-400} * (Salinity_{surface\ sample}/Salinity_{200-400})] - TA_{200-400} \quad (5)$$

16  $DIC_{200-400}$ ,  $TA_{200-400}$ , and  $Salinity_{200-400}$  are the average values for samples collected from 200-  
17 400 m calculated at each station.

18 The partial derivatives quantify the change in  $\Omega_{Ar}$  per unit change in DIC, TA, temperature, and  
19 salinity respectively. To determine the partial derivatives, we calculate  $\Omega_{Ar}$  for all hydrocast  
20 samples within the upper 10 m using DIC, TA, temperature, and salinity as input parameters. We  
21 recalculate  $\Omega_{Ar}$  after independently increasing DIC, TA, temperature, and salinity by one unit.  
22 The partial derivatives are the average difference between the initial  $\Omega_{Ar}$  and the recalculated  
23  $\Omega_{Ar}$ .

24 We use the same equations to evaluate the relative importance of DIC, TA, temperature, and  
25 salinity on the variability of  $\Omega_{Ar}$  from  $75^{\circ}\text{S}$  to  $55^{\circ}\text{S}$ . For the  $\Delta$  terms, we calculate the change in  
26 sDIC, sTA, temperature, and salinity from the mean of the first 6 underway measurements at

1 75°S. For Eq. 4 and Eq. 5, instead of using DIC, TA, and salinity values from 200-400 m, we use  
2 the mean of the first 6 underway measurements at 75°S.

3

## 4 **4 Results and Discussion**

### 5 **4.1 $\Omega$ in the Ross Sea**

6 ~~We define the area west of 171°E as the western region and the area between 171 and 180°E as~~  
7 ~~the central region. This demarcation is similar to regions defined by Sweeney et al. (2000a) and~~  
8 ~~roughly traces the western boundary between sea ice and open water when the Ross Sea polynya~~  
9 ~~is opening during austral spring (Fig. 2a).~~

10 ~~Surface water salinity is lower in the western region ( $33.79 \pm 0.27$ ) than the central~~  
11 ~~region ( $34.11 \pm 0.10$ ) (Fig. 2b). While sea ice advects northwards in the central region as the~~  
12 ~~Ross Sea polynya forms, in the western region much of the sea ice melts in place lowering the~~  
13 ~~surface salinity and increasing stratification. Monthly Aqua-MODIS chlorophyll concentration~~  
14 ~~data shows that the highest chlorophyll concentrations during February 2013 are in the western~~  
15 ~~region (Fig. 2c). Arrigo et al. (1999) also observed that diatom blooms in the highly stratified~~  
16 ~~western region peak during the early autumn — 6 weeks after the main *Phaeocystis antarctica*~~  
17 ~~bloom in the central Ross Sea.~~

18 ~~Surface~~Underway TA values range from 2268 to 2346  $\mu\text{mol kg}^{-1}$  (mean =  $2314 \pm 16 \mu\text{mol kg}^{-1}$ ).  
19 Since TA strongly covaries with salinity ( $R^2=0.86$ , residual  $\pm 6 \mu\text{mol kg}^{-1}$ ), the lowest TA values  
20 are located in the ~~western region~~west where the salinity is lowest (Fig. 1b). Values of sTA range  
21 from 2336 to 2386  $\mu\text{mol kg}^{-1}$  (mean =  $2360 \pm 7 \mu\text{mol kg}^{-1}$ ) and are influenced by  
22 calcification/dissolution as well as phytoplankton photosynthesis since one unit of nitrate  
23 drawdown increases TA by one unit (Brewer and Goldman, 1978) (Fig. ~~2d~~1d).

24 Surface  $\text{pCO}_2$  values range from 162 to 354  $\mu\text{atm}$  (Fig 2e). ~~Surface  $\text{pCO}_2$  values~~and  
25 ~~the western region ( $238 \pm 34 \mu\text{atm}$ ) compared to the central region ( $319 \pm 16 \mu\text{atm}$ ) due to~~  
26 ~~greater-late season~~ phytoplankton photosynthesis (Fig 1e)in the west. Surface  $\Omega_{\text{Ar}}$  ~~values~~ranges  
27 from 1.40 to 2.42 and  $\Omega_{\text{Ca}}$  ranges from 2.24 to 3.89 (Fig. 2f). The highest  $\Omega_{\text{Ar}}$  values are also  
28 located in the west ~~western region ( $1.94 \pm 0.18$ ,  $\Omega_{\text{Ca}} = 3.09 \pm 0.30$ ) compared to the central~~

1 | ~~region ( $1.58 \pm 0.09$ ,  $\Omega_{Ar} = 2.52 \pm 0.14$ ). Greater phytoplankton~~ Phytoplankton photosynthesis in  
2 | ~~the western region~~ increases  $\Omega$  by both decreasing DIC and increasing TA.

3 | Spatial and temporal variations in surface water  $\Omega_{Ar}$  are mainly controlled by sDIC in the Ross  
4 | Sea (Eq. 2, Fig. 3). The concentration of sDIC decreased by  $58 \pm 20 \mu\text{mol kg}^{-1}$  from a winter  
5 | value, causing  $\Omega_{Ar}$  to increase by  $0.5 \pm 0.2$ . In addition, sTA increased by  $11 \pm 7 \mu\text{mol kg}^{-1}$   
6 | during the preceding summer months, causing  $\Omega_{Ar}$  to increase by  $0.1 \pm 0.1$ . Although there was a  
7 | significant reduction in salinity compared to winter values ( $0.7 \pm 0.3$ ),  $\Omega_{Ar}$  only decreased by  $\sim$   
8 | 0.01 due to this freshening since both DIC and TA concentrations were reduced. Lastly, the  
9 | effect of temperature on  $\Omega_{Ar}$  was negligible since the Ross Sea only experiences a  $2^\circ\text{C}$  seasonal  
10 | change in SSTs (Sweeney, 2003).

11 | Two processes can reduce sDIC: calcification and phytoplankton photosynthesis. To evaluate  
12 | the importance of calcification, we use time dependent changes in potential alkalinity  
13 | (~~pTA-PALK =~~, defined as  $\text{sNitrate} + \text{sTA}$ ) from a winter value ( $2367 \pm 3 \mu\text{mol kg}^{-1}$ , defined as  
14 | average value for all samples between 200–400 m). While TA will increase during  
15 | photosynthesis due to nitrate drawdown, ~~pTA-PALK~~ will be conserved. Therefore, changes in  
16 | ~~pTA-PALK~~ can be attributed to calcification and dissolution. The average  ~~$\Delta\text{pTA}-\Delta\text{PALK}$~~  from a  
17 | winter concentration is negligible ( $0 \pm 5 \mu\text{mol kg}^{-1}$ ); therefore, calcification appears to be  
18 | insignificant and the increase in sTA from winter conditions is largely driven by nitrate  
19 | drawdown during photosynthesis. Earlier studies found that calcification contributed to only  $\sim$   
20 | 5% of the total seasonal DIC drawdown (Bates et al., 1998; Sweeney et al., 2000a; ~~Bates et al.,~~  
21 | ~~1998~~). Therefore, we argue that photosynthesis exerts the dominant control on sDIC, sTA, and  
22 |  $\Omega_{Ar}$ . While the highest  $\Omega_{Ar}$  value that we observed was 2.4, values up to  $\sim 4$  have been observed  
23 | during Dec-Jan (McNeil et al., 2010). By the time we arrived in the Ross Sea, surface sDIC  
24 | concentrations would have already increased relative to the summer due to enhanced air-sea  
25 |  $\text{CO}_2$  fluxes (Arrigo and Van Dijken, 2007), deepening of the mixed layer (Sweeney, 2003), and  
26 | remineralization of organic carbon (Sweeney et al., 2000b).

27 | Mattsdotter Björk et al. (2014) also argue that phytoplankton photosynthesis is the major control  
28 | on surface water  $\Omega_{Ar}$  variability between the Ross Sea and the Antarctic Peninsula based upon  
29 | the covariance of  $\Omega_{Ar}$  and chlorophyll-a. The largest contributor to seasonal  $\Omega_{Ar}$  change in the  
30 | Chukchi Sea in the Arctic is also phytoplankton photosynthesis (Bates et al., 2013). However,

1 unlike the Ross Sea, numerous studies have also demonstrated aragonite undersaturation of  
2 surface waters in parts of the Arctic due to sea ice melt and river runoff ~~leads to significant~~  
3 ~~reductions in  $\Omega_{Ar}$~~  (Chierici and Fransson, 2009; Yamamoto et al., 2009; Robbins et al., 2013).

#### 5 4.2 $\Omega$ in the Southern Ocean

6 The spatial changes in  $\Omega_{Ar}$ , SST,  $pCO_2$ , and ~~particulate organic matter (POC)~~ between 75°S and  
7 55°S are shown in Fig. 4. We also include the mean location of the fronts from Sokolov and  
8 Rintoul (2009) as they intersect our cruise track. The lowest  $\Omega_{Ar}$  value is 1.25 ( $\Omega_{Ca} = 2.00$ ) at  
9 75°S, corresponding with the highest  $pCO_2$  of  $\sim 396 \mu atm$ .  $\Omega_{Ar}$  increases along the transect to  
10 reach a maximum of 1.93 ( $\Omega_{Ca} = 3.04$ ) at 55°S. The ~~changes in  $\Omega_{Ar}$  are not always monotonic~~  
11 ~~rate of increase is not always linear.~~ In two regions cChanges in  $\Omega_{Ar}$  can be attributed to enhanced  
12 primary production. ~~sometimes correspond to drops in  $pCO_2$ . For instance, B~~between 74°S and  
13 73°S,  $\Omega_{Ar}$  first increases and then decreases by  $\sim 0.1$ . This corresponds with a  $40 \mu atm$  drop and  
14 then rise in  $pCO_2$ . Given that SST is constant, this localized increase in  $\Omega_{Ar}$  is likely due to  
15 phytoplankton photosynthesis. This region may be along the Antarctic Slope Front that is known  
16 for higher biological activity (Jacobs, 1991). There is another step in  $\Omega_{Ar}$  from  $\sim 1.4$  to  $\sim 1.5$   
17 between ~~67.568°S~~ and ~~67.66°S~~ across the SACCF-N. This step also corresponds with a decrease  
18 in  $pCO_2$  from  $\sim 370$  to  $\sim 340 \mu atm$ , ~~likely due to phytoplankton photosynthesis~~. Elevated POC  
19 concentrations between the SACCF-N and the PF-M correspond with these and lower  $pCO_2$   
20 values ~~around the PF and again~~ indicate enhanced phytoplankton photosynthesis. Ruben (2003)  
21 also found that  $pCO_2$  is reduced south of the PF (170°W) due to primary production.

22 To further gain insight into why  $\Omega_{Ar}$  increases along our transect, wWe quantify the contribution  
23 of changing sDIC (calculated from TA and  $pCO_2$ ), sTA, SST, and salinity to changing  $\Omega_{Ar}$  along  
24 the transect (Fig. 5a). The dominant control is declining sDIC<sub>calc</sub> from  $\sim 2240$  to  $\sim 2140 \mu mol kg^{-1}$   
25 between 75°S and 55°S, which causes  $\Omega_{Ar}$  to increase by 0.87 if sTA, SST, and salinity are held  
26 constant (Fig. 6). Declining sTA from  $\sim 2340$  to  $\sim 2310 \mu mol kg^{-1}$  partially counters the influence  
27 of sDIC<sub>calc</sub> and reduces  $\Omega_{Ar}$  by 0.28. The influences of SST and salinity on  $\Omega_{Ar}$  are minimal.

28  $\Omega_{Ar}$  variability is driven almost entirely by changes in sDIC<sub>calc</sub>, ~~from 75°S to the PF-S~~. Between  
29 the PF-S and the SAF-N, variability in  $\Omega_{Ar}$  is influenced by the opposing effects of sDIC<sub>calc</sub> and  
30 sTA. The TA:DIC<sub>calc</sub> ratio and  $\Omega_{Ar}$  are constant between the PF-S and ~~60°S~~ the SAF-S since both

1 | sDIC<sub>calc</sub> and sTA decrease at the same rate (Fig. 5b). Between 60°S the SAF-S and the SAF-N,  
2 |  $\Omega_{Ar}$  increases since sDIC<sub>calc</sub> declines faster than sTA (Fig. 5b). North of the SAF-N,  $\Omega_{Ar}$   
3 | variability is again driven by sDIC<sub>calc</sub>:  $\Omega_{Ar}$  increases due to a decrease in sDIC<sub>calc</sub> while sTA  
4 | remains constant.

5 | We examine possible controls on sDIC<sub>calc</sub> along the transect. The concentration of sDIC<sub>calc</sub> is  
6 | highest south of the PF-S due to upwelling of CDW (Fig. 6a). To evaluate the properties of  
7 | CDW, we use data from the 2011 Repeat Hydrography Cruise SO4P, which is part of the U.S.  
8 | Climate Variability and Predictability (CLIVAR) program (Swift and Orsi, 2012) (available at  
9 | <http://www.clivar.org/resources/data/hydrographic>). We only use data from hydrocasts located  
10 | between 168°E – 73°W where the bottom depth is >1000 m (Fig. 4b2b). We reject the data from  
11 | hydrocast 46(B) where the deep DIC data below 200 m is ~ 30  $\mu\text{mol kg}^{-1}$  higher than the rest of  
12 | the stations. Following Sweeney (2003), CDW is defined as centered on the level of maximum  
13 | temperature below 150 m.

14 | From this CLIVAR dataset, CDW has a sDIC value of  $2243 \pm 3 \mu\text{mol kg}^{-1}$ . Between 75°S and  
15 | 74°S, sDIC<sub>calc</sub> concentration of surface water is also  $2243 \pm 5 \mu\text{mol kg}^{-1}$ , indicating little  
16 | modification to CDW and consistent with the observation that this region was covered by sea ice  
17 | even during the summer of 2013. At 74°S sDIC<sub>calc</sub> drops to ~2220  $\mu\text{mol kg}^{-1}$  and at by 67.566°S,  
18 | across the SACCF-N, sDIC<sub>calc</sub> drops to ~2200  $\mu\text{mol kg}^{-1}$ . The main driver of This 40  $\mu\text{mol kg}^{-1}$   
19 | decrease in sDIC<sub>calc</sub> between Antarctica and the PF-S is consistent with the observed drops in  
20 | pCO<sub>2</sub> that we attributed to likely photosynthesis. Ruben et al. (1998) also observed a 30-50  $\mu\text{mol}$   
21 |  $\text{kg}^{-1}$  decrease in sDIC at 67°S in Pacific Antarctic waters between winter and summer that they  
22 | attribute to primary productivity.

23 | sDIC<sub>calc</sub> continues to drop from ~2220  $\mu\text{mol kg}^{-1}$  at the PF-S to ~2140  $\mu\text{mol kg}^{-1}$  at 55°S,  
24 | consistent with surface DIC measurements between 70°S and 40°S compiled by McNeil et al.  
25 | (2007). There are multiple factors likely responsible for this decrease in sDIC<sub>calc</sub>. Both satellite  
26 | (Arrigo et al., 2008) and in situ measurements (Reuer et al., 2007) show that annual primary  
27 | productivity increases from south to north in the Southern Ocean. In addition, surface waters  
28 | north of the PF advect northwards and accumulate a sDIC deficit. Finally, warmer water holds  
29 | less DIC while in equilibrium with the atmosphere. There is little net air-sea CO<sub>2</sub> flux between

1 75°S and 55°S (except for net efflux at 60°S) since warming and increased biological production  
2 compensate each other (Takahashi et al., 2012).

3 We also examine possible controls on sTA concentrations along the transect. The concentration  
4 of sTA is also highest south of the PF-S due to upwelling of CDW. Based off the CLIVAR  
5 dataset, the sTA of CDW is  $2334 \pm 3 \mu\text{mol kg}^{-1}$ . The sTA of sSurface water between 74°S and the  
6 PF-S has a relatively constant sTA concentration of  $\sim 2340 \mu\text{mol kg}^{-1}$ , slightly higher than its  
7 CDW source (Fig. 6b). Nitrate drawdown during photosynthesis may explain the elevated sTA.  
8 Between 75°S and 74°S, sTA exceeds  $2360 \mu\text{mol kg}^{-1}$ . One possible explanation is that ikaite  
9 ( $\text{CaCO}_3 \cdot 6\text{H}_2\text{O}$ ), a mineral that has been observed directly and indirectly to precipitate in  
10 Antarctic sea ice (Dieckmann et al., 2008; Fransson et al., 2011), dissolved into surface waters  
11 during the summer causing sTA concentrations to increase. Between the PF-S and SAF-N, sTA  
12 drops to  $2310 \mu\text{mol kg}^{-1}$  where the concentrations level off. This drop appears to be in part due to  
13 the mixing of two end member water masses, AASW south of the PF-S and subtropical  
14 Subantarctic surface water north of the SAF-N. The decreasing sTA is consistent with the  
15 suggestion of Millero et al. (1998) that a negative linear relationship between sTA and SST is  
16 due to colder water being indicative of greater upwelling of TA rich water.

17 This dataset supports the argument that increased upwelling of CDW from strengthening  
18 westerly winds will increase OA in the Southern Ocean (Lenton et al., 2009). While the TA:DIC  
19 ratio for CDW is  $1.040 \pm 0.002$ , the TA:DIC<sub>calc</sub> ratio for surface waters between 75°S and the  
20 PF-S ranges from 1.046 to 1.064 (Fig. 5b). Therefore increased upwelling will lower the TA:DIC  
21 ratio and cause  $\Omega_{\text{Ar}}$  to decrease.

22

### 23 **4.3 Estimate of wintertime surface $\Omega_{\text{Ar}}$ values in the Ross Sea**

24 Efforts to predict winter  $\Omega_{\text{Ar}}$  undersaturation in the Ross Sea are complicated by the complete  
25 lack of carbon system measurements from the winter months in the Ross Sea.

26

27 McNeil et al. (2010) estimated winter surface water  $\Omega_{\text{Ar}}$  by using the lowest observed  $\Omega_{\text{Ar}}$  value  
28 from early spring when the Ross Sea is still covered by sea ice. They used mid October and early  
29 November carbon system measurements from the Joint Global Ocean Flux Study (JGOFS)

1 (Sweeney et al., 2000b). Although sea ice algae productivity peaks in November, their impact on  
2 water column DIC concentrations is likely to be negligible (Saenz and Arrigo, 2014). McNeil et  
3 al. (2010) found that early spring surface water  $\Omega_{Ar}$  was  $\sim 1.2$ . There was a single  $\Omega_{Ar}$  value  $< 1.1$   
4 that they used as an initial condition along with the IPCC US92a scenario to predict that surface  
5 waters of the Ross Sea could begin to experience seasonally undersaturated conditions with  
6 respect to aragonite as early as 2015 if full equilibrium with rising atmospheric  $\text{CO}_2$  is achieved.  
7 Based on a three-dimensional Coupled Ice, Atmosphere, and Ocean model (Arrigo et al., 2003,  
8 Tagliabue and Arrigo, 2005), McNeil et al. (2010) argued that only 35% of the atmospheric  $\text{CO}_2$   
9 signal equilibrates with Ross Sea surface waters due to sea ice, upwelling of CDW, and short  
10 residence times, thereby delaying the onset of aragonite undersaturation until 2045. Decadal  
11 wintertime surface carbon system measurements do not exist to directly validate this  
12 disequilibrium assumption. In addition, McNeil et al. (2010) would inaccurately predict when the  
13 Ross Sea would become undersaturated with respect to aragonite if the minimum wintertime  
14 surface  $\Omega_{Ar}$  value used was low due to measurement error.

15 To independently calculate  $\Omega_{Ar}$  from early spring surface waters, we use the LDEO  $\text{pCO}_2$   
16 measurements from November 1994, 1997, 2005, and 2006 that are from the Ross Shelf (defined  
17 by the 1000m isopleth) and are south of  $74^\circ\text{S}$  (Fig. 7a). The earliest  $\text{pCO}_2$  measurements are  
18 from 16 Nov 1994, 17 Nov 1997, 6 Nov 2005, and 13 Nov 2006 when much of the Ross Sea is  
19 still covered in sea ice. The earliest measurements from 2005/06 are more likely to represent  
20 winter conditions since they are from  $74^\circ\text{S}$  as the NBP entered the Ross Sea. Conversely, the  
21 earliest measurements from 1994/97 are from the  $76.5^\circ\text{S}$  line, close to where the Ross Sea  
22 polynya opens up from.

23 We calculate wintertime TA in the Ross Sea by establishing a salinity-TA relationship using data  
24 from Bates et al. (1998), Sweeney et al. (2000b), and our own hydrocast TA measurements from  
25 the upper 10 m (Fig. 7bA1). Since one unit of nitrate drawdown increases TA by one unit, the  
26 TA measurements are adjusted to winter nitrate concentrations of  $29 \mu\text{mol kg}^{-1}$  (the mean nitrate  
27 concentration between 200-400 m from our cruise). The relationship between TA and salinity is  
28 consistent among these independent datasets and the standard deviation of the residuals for TA is  
29  $\pm 5 \mu\text{mol kg}^{-1}$ .

1 We calculate historical  $\Omega_{Ar}$  using historical  $pCO_2$  measurements, ~~salinity derived TA-calculated~~  
2 ~~from salinity~~, SST, and salinity. Phosphate and silicate are set to the winter values of  $2.1 \mu mol$   
3  $kg^{-1}$  and  $79 \mu mol kg^{-1}$  respectively. The ~~thermosalinograph (TSG)~~ salinity data from the  
4 historical  $pCO_2$  measurements appears reasonable and is uncalibrated. While the largest offset in  
5 TSG salinity compared with Autosol measurements is 0.3, such error is not typical. ~~For instance,~~  
6 ~~on our cruise the difference between TSG and Autosol measurements is less than 0.02.~~ To test  
7 the possible impact of a poor salinity calibration, we recalculate  $\Omega_{Ar}$  for all  $pCO_2$  measurements  
8 after increasing salinity by 0.3. TA calculated from the observed TA-salinity relationship  
9 increases by  $\sim 21 \mu mol kg^{-1}$  and  $\Omega_{Ar}$  increases by  $0.024 \pm 0.003$ .

10 The lowest  $\Omega_{Ar}$  measurements are 1.24 in 1994, 1.25 in 1997, 1.22 in 2005, and 1.20 in 2006  
11 (Fig. ~~7e7b~~). Although  $\Omega_{Ar}$  declines from 1994 to 2006, we have low confidence in any trend due  
12 to spatial-temporal sampling biases. The lowest  $\Omega_{Ar}$  values are consistently between 1.2 and 1.3  
13 as the ship crossed sea ice covered regions and open water that had experienced DIC drawdown.  
14 With the exception of a single measurement, the lowest 1996/97  $\Omega_{Ar}$  values from McNeil et al.  
15 (2010) are also  $\sim 1.2$ . The similarity between the  $\Omega_{Ar}$  values reported by McNeil et al. (2010)  
16 from 1996/97 and our 2005/06 values is consistent with their delayed acidification hypothesis.

17 A simple calculation also suggests that wintertime  $\Omega_{Ar}$  values may be closer to 1.2 than 1.1. If  
18 salinity is 34.5, approximately the mean salinity of the water column, TA would be  $2339 \mu mol$   
19  $kg^{-1}$  based on the observed TA-salinity linear relationship. Sweeney (2003) estimates winter  
20  $pCO_2$  values of  $\sim 425 \mu atm$  based on deep  $pCO_2$  measurements made during early spring. Setting  
21 salinity to 34.5, TA to  $2339 \mu mol kg^{-1}$ ,  $pCO_2$  to  $425 \mu atm$ , temperature to  $-1.89$ , silicate to  $79$   
22  $\mu mol kg^{-1}$ , and phosphate to  $2.1 \mu mol kg^{-1}$  yields a  $\Omega_{Ar}$  value of 1.22.

23 Although  $pCO_2$  measurements of surface waters colder than  $-1.75^\circ C$  south of  $60^\circ S$  typically  
24 reach  $\sim 410 \mu atm$  by September, Takahashi et al. (2009) present a few measurements of  $\sim 450$   
25  $\mu atm$ . Even if  $pCO_2$  reaches  $450 \mu atm$  during winter in the Ross Sea,  $\Omega_{Ar}$  would be 1.16 (with  
26 salinity at 34.5 and TA at  $2339 \mu mol kg^{-1}$ ). In order to obtain  $\Omega_{Ar}$  of 1.1,  $pCO_2$  would need to be  
27  $\sim 480 \mu atm$ , a value that appears unreasonably high given the available datasets from the Ross  
28 Sea.

29 McNeil et al. (2010) calculated the  $\Omega_{Ar}$  of water arriving onto the Ross Shelf following the  
30 recipes of Jacobs and Fairbanks (1985): 50% CDW, 25% Tmin water (minimum temperature in



1 upper 100 m), and 25% AASW. To calculate the  $\Omega_{Ar}$  of these three source water masses, they  
2 used hydrocast temperature, salinity, and DIC data collected during the austral winter of 1994  
3 from north of the Ross Shelf as described in Sweeney (2003). They calculated that the average  
4  $\Omega_{Ar}$  of incoming water would be 1.08.

5 We independently calculate  $\Omega_{Ar}$  of incoming water using the 2011 CLIVAR hydrocast data from  
6 north of the Ross Shelf between 168°E – 73°W as described earlier (Fig. 4b2b). The  $\Omega_{Ar}$  of water  
7 in the upper 100 m (AASW and Tmin) from the CLIVAR dataset is  $1.36 \pm 0.13$  and the  $\Omega_{Ar}$  of  
8 CDW (maximum temperature below 150 m) is  $1.18 \pm 0.03$  (Fig. 7dA2). Even if 100% of the  
9 incoming water onto the Ross Shelf is CDW, the  $\Omega_{Ar}$  of this incoming water would be  
10 ~~significantly~~ greater than 1.08. While most properties of CDW are similar between the 2011  
11 CLIVAR data and the 1994 data used by McNeil et al. (2010), the TA of CDW from the  
12 CLIVAR dataset is  $18 \mu\text{mol kg}^{-1}$  higher (Table 2).

13 Another approach to estimate the  $\Omega_{Ar}$  of winter surface waters is to use the properties of water  
14 below 200 m. For the TRACERS data, sTA below 200 m is  $2338 \pm 2 \mu\text{mol kg}^{-1}$ . For the JGOFS  
15 autumn cruise (NBP 97-3) sTA below 200 m is  $2339 \pm 2 \mu\text{mol kg}^{-1}$ . Using the CLIVAR dataset,  
16 sTA of CDW from off the Ross Shelf is  $2334 \pm 3 \mu\text{mol kg}^{-1}$ . This consistency between  
17 independent datasets suggests that we can accurately estimate winter TA in the Ross Sea.

18 The range in sDIC below 200m is much greater than that for sTA (Table 2). The lowest value is  
19  $2220 \pm 5 \mu\text{mol kg}^{-1}$  from our cruise and the highest is  $2237 \pm 3 \mu\text{mol kg}^{-1}$  from the summer  
20 JGOFS cruise (NBP 97-01). This range in sDIC concentrations below 200 m is not surprising  
21 given that sDIC concentrations vary across the input water masses. In addition, sDIC  
22 concentrations below 200 m will be influenced by carbon export particularly in summer and  
23 early autumn and over multiple seasons' air to sea flux of  $\text{CO}_2$ .

24 Assuming that deep water concentrations of TA and DIC are relatively unmodified following  
25 wintertime deep convective mixing, we estimate the  $\Omega_{Ar}$  of winter surface water by setting TA to  
26  $2338 \mu\text{mol kg}^{-1}$ , salinity to 34.5, temperature to  $-1.89^\circ\text{C}$ , phosphate to  $2.1 \mu\text{mol kg}^{-1}$ , and silicate  
27 to  $79 \mu\text{mol kg}^{-1}$ . If DIC concentrations are  $2220 \mu\text{mol kg}^{-1}$ ,  $\Omega_{Ar}$  would be 1.37. If sDIC  
28 concentrations are  $2237 \mu\text{mol kg}^{-1}$ ,  $\Omega_{Ar}$  would be 1.24 and  $\text{pCO}_2$  would be 417  $\mu\text{atm}$ .

29 These results are consistent with a study by Matson et al. (2014) where early spring  $\Omega_{Ar}$  at 20 m  
30 depth calculated using pH and salinity derived TA was 1.2 – 1.3 from Hut Point (bottom depth >

1 200 m) and Cape Evans (bottom depth < 30 m) in McMurdo Sound. In Prydz Bay, the lowest  
2 measured winter surface  $\Omega_{Ar}$  values were also ~ 1.2 during for both 1993-95 (Gibson and Trull,  
3 1999; McNeil et al., 2011) in Prydz Bay (McNeil et al., 2014) and 2010-11 (Roden et al., 2013).  
4 Weeber et al. (2015) using hydrocast data estimated that the  $\Omega_{Ar}$  of Winter Water in the Weddell  
5 Sea was ~ 1.3. In the Mertz Polynya, the lowest  $\Omega_{Ar}$  value at 100 m (below the mixed layer) was  
6 1.2 (Shadwick et al., 2013). In Arthur Harbor on the western Antarctic Peninsula the lowest  
7 winter surface  $\Omega_{Ar}$  value was 1.31 (Schram et al., 2015).

8 A few studies find Antarctic winter  $\Omega_{Ar}$  values for surface water below 1.2. Hauri et al. (2015)  
9 used LDEO pCO<sub>2</sub> measurements and predicted TA from salinity to estimate winter  $\Omega_{Ar}$  values of  
10 surface water in the western Antarctic Peninsula. They found that 20% of  $\Omega_{Ar}$  values were below  
11 1.2 during the spring and winter, with a few winter values near undersaturation. It is not  
12 surprising that winter surface  $\Omega_{Ar}$  values are lower in the Antarctic Peninsula than the Ross Sea  
13 given less sea ice in the Peninsula. In another study, Kapsenberg

14 Hofmann et al. (2015) report  $\Omega_{Ar}$  at 18 m depth (bottom depth < 30 m) at two coastal sites in  
15 McMurdo Sound, the Jetty and Cape Evans, for Dec-May and Nov-June respectively using pH  
16 and salinity derived TA as input variables. The lowest  $\Omega_{Ar}$  observations were from May at both  
17 sites and were 1.22 and 0.96 at the Jetty and Cape Evans. The maximum calculated pCO<sub>2</sub> was  
18 559 at Cape Evans. The low  $\Omega_{Ar}$  and high calculated pCO<sub>2</sub> values measured by Hofmann  
19 Kapsenberg et al. (2015) may represent differences between coastal and open ocean systems—  
20 there may be a coastal amplification signal when sinking organic matter hits a shallow bed.  
21 Another possibility is that their carbon system time series, particularly at Cape Evans, is  
22 inaccurate. After conditioning and calibrating their pH measurements using discrete water  
23 samples, for logistical reasons Hofmann-Kapsenberg et al. (2015) could not collect additional  
24 validation samples during deployment or measure multiple carbon system parameters for  
25 crosscheck. Although the SeaFET pH sensors that they used are generally stable, they can drift  
26 (Bresnahan et al., 2014). Hofmann-Kapsenberg et al. (2015) have no means to assess possible pH  
27 sensor drift.

28 Following McNeil et al. (2010) and a Representative Concentration Pathway (RCP8.5) scenario  
29 (Meinshausen et al., 2011), we use the lowest  $\Omega_{Ar}$  values from 2006 ( $\Omega_{Ar} = 1.20$ , pCO<sub>2</sub> =  
30 428  $\mu$ atm, TA = 2328  $\mu$ mol kg<sup>-1</sup>, salinity = 34.33, SST = -1.87°C, phosphate = 2.1  $\mu$ mol kg<sup>-1</sup>,

1 silicate =  $79 \mu\text{mol kg}^{-1}$ ) to assess when the Ross Sea could become corrosive to aragonite. While  
2 shelf water salinity in the Ross Sea has declined by  $0.03 \text{ decade}^{-1}$  from 1958 to 2008 (Jacobs and  
3 Giulivi, 2010), we show that such rates of change will have inconsequential effects on  $\Omega_{\text{Ar}}$ . For  
4 equilibrium conditions, surface waters in the Ross Sea would become corrosive to aragonite by  
5 2040 (2092 for calcite) when atmospheric  $\text{CO}_2$  concentrations exceed 485 ppm. In the  
6 disequilibrium scenario (McNeil et al., 2010), surface aragonite undersaturation state would  
7 occur by 2071 (2185 for calcite) when atmospheric  $\text{CO}_2$  concentrations exceed 677 ppm.

8 Mattsdotter Björk et al. (2014) also predicted the onset of summertime aragonite in the Ross Sea.  
9 Their lowest  $\Omega_{\text{Ar}}$  value was also  $\sim 1.2$  and they estimated onset of undersaturation between 2026  
10 and 2030 by increasing DIC by  $10 \mu\text{mol kg}^{-1}$  per decade. This approach does not take into  
11 account air-sea  $\text{CO}_2$  disequilibrium. In contrast, Hauck et al. (2010) found that only 3 – 5  $\mu\text{mol}$   
12  $\text{kg}^{-1}$  of anthropogenic carbon accumulated per decade between 1992 and 2008 in shelf water of  
13 the Weddell Sea. In short, our analysis suggests that it may be possible to prevent future winter  
14 aragonite undersaturation of surface waters in the Ross Sea. For instance,  $\text{CO}_2$  concentrations  
15 never exceed 543 ppm in the  $\text{CO}_2$  stabilization scenario RCP4.5 (Meinshausen et al., 2011).

16 If the Ross Sea experiences aragonite undersaturation during winter in the future, live pteropod  
17 shells would start dissolving, making them more vulnerable to predation and bacterial infection  
18 (Bednaršek et al., 2012, 2014). In particular, pteropod larvae develop during the winter/spring  
19 (Gannefors et al., 2005; Hunt et al., 2008) and their shells have been shown to completely  
20 dissolve within weeks of exposure to aragonite undersaturation (Comeau et al., 2010). Declines  
21 in pteropod populations may reduce carbon export (Manno et al., 2010) and could have dramatic  
22 ecological effects up the food web.

23 Antarctic deep sea hydrocorals may also decline or disappear at the onset of aragonite  
24 undersaturation (Shadwick et al., 2014). In addition, the shells of post-mortem bivalves and  
25 brachiopods show significant dissolution within two months of exposure to undersaturated  
26 conditions, although live organisms may be able to compensate for this dissolution (McClintock  
27 et al., 2009). For instance, Cummings et al. (2011) show that the Antarctic bivalve *Laternula*  
28 *elliptica* can increase calcification in undersaturated conditions. However, the associated energy  
29 costs may be difficult to maintain over the long term, especially for larvae. Stumpp et al. (2012)  
30 shows that while echinoid larvae can maintain calcification in high  $\text{pCO}_2$  treatments, increased

energetic costs reduce growth rates and ultimately increase mortality. Larvae of the Antarctic sea urchin *Sterechinus neumayeri* and seastar *Odontaster validus* are smaller and exhibit abnormal development under elevated pCO<sub>2</sub> treatments (Byrne et al., 2013; Gonzalez-Bernat et al., 2013; Yu et al., 2013). In addition, the synergistic effects of warming and OA could impact echinoderm fertilization and embryo development (Ericson et al., 2012). Although it is not clear to what extent species may acclimatize or adapt (e.g. Suckling et al., 2015), the onset of aragonite undersaturation during winter months may have profound impacts on the Ross Sea ecosystem.

Formatted: Font: Italic

## 5 Conclusions

Formatted: Font: German (Germany)

Formatted: Heading 1

Our study demonstrates the possibility of setting up underway TA measurement systems. Although our system was relatively unattended, carbon system crosschecks and comparisons between hydrocast and underway data indicate that our measurements were accurate. Similar underway TA systems could be set up on scientific vessels and ships of opportunity in undersampled regions of the world's oceans.

We find that the seasonal increase in  $\Omega_{Ar}$  in the Ross Sea by early autumn is driven almost entirely by phytoplankton photosynthesis. In the Southern Ocean between the Ross Sea and Chile we find that  $\Omega_{Ar}$  also increases mainly due to declining DIC<sub>calc</sub>, although declining TA partially counters the influence of declining DIC<sub>calc</sub>. The influences of SST and salinity on  $\Omega_{Ar}$  are minimal in the Ross Sea and on our Southern Ocean transect.

We establish a salinity-TA relationship for the winter that is consistent across independent datasets. Using historical pCO<sub>2</sub> measurements from early spring along with TA predicted from salinity, ~~In conclusion,~~ we argue that it is unlikely that the Ross Sea actually experienced winter surface  $\Omega_{Ar}$  values of ~1.1 during 1996 (as per McNeal et al., 2010) and that a  $\Omega_{Ar}$ -value of ~1.2 may more accurately represent current winter conditions.

Since predictions are sensitive to current surface wintertime  $\Omega_{Ar}$  values as well as the extent of disequilibrium, highly accurate ~~over-determined~~ carbon system measurements from the winter are crucial. It is also essential to measure more than two carbon system parameters for

1 [crosscheck. For instance, pH and pCO<sub>2</sub> sensors on moorings and floats could be used with TA](#)  
2 [predicted from salinity to calculate Ω during the winter.](#)

3 [Our analysis indicates that the Ross Sea will not experience aragonite undersaturation until the](#)  
4 [year 2070 following RCP8.5. In some CO<sub>2</sub> stabilization scenarios, including RCP4.5](#)  
5 [\(Meinshausen et al., 2011\), the Ross Sea may avoid becoming corrosive to aragonite.](#)

## 8 Acknowledgements

9 This work was supported by the U.S. NSF (OPP-1142044 to R. B. D) and a NSF Graduate  
10 Research Fellowship grant (DGE-114747 to H. B. D). We thank the captain and crew of the *R/V*  
11 *Nathaniel B. Palmer*. We ~~thank~~ [are grateful to](#) S. Bercovici for the nitrate data. [The comments of](#)  
12 [two anonymous reviewers greatly improved this paper.](#)

## 14 References

15 Accornero, A., Manno, C., Esposito, F. and Gambi, M. C.: The vertical flux of particulate matter  
16 in the polynya of Terra Nova Bay. Part II. Biological components, *Antarct. Sci.*, 15, 175–188,  
17 doi:10.1017/S0954102003001214, 2003.

18 Andersson, A. J., Mackenzie, F. T. and Gattuso, J.-P.: Effects of ocean acidification on benthic  
19 processes, organisms, and ecosystems, in: *Ocean Acidification*, edited by: Gattuso, J.-P. and  
20 Hanson, L., Oxford University Press, New York, 122-153, 2011.

21 Archer, D., Eby, M., Brovkin, V., Ridgwell, A., Cao, L., Mikolajewicz, U., Caldeira, K.,  
22 Matsumoto, K., Munhoven, G., Montenegro, A. and Tokos, K.: Atmospheric Lifetime of Fossil  
23 Fuel Carbon Dioxide, *Annu. Rev. Earth Planet. Sci.*, 37, 117–134,  
24 doi:10.1146/annurev.earth.031208.100206, 2009.

25 Arrigo, K. R. and McClain, C. R.: Spring Phytoplankton Production in the Western Ross Sea,  
26 *Science*, 266, 261–263, doi:10.1126/science.266.5183.261, 1994.

27 Arrigo, K. R. and van Dijken, G. L.: Phytoplankton dynamics within 37 Antarctic coastal  
28 polynya systems, *J. Geophys. Res.*, 108, 3271, doi:10.1029/2002JC001739, 2003.

1 [Arrigo, K. R. and Van Dijken, G. L.: Annual changes in sea-ice, chlorophyll a, and primary](#)  
2 [production in the Ross Sea, Antarctica, Deep. Res. Part II Top. Stud. Oceanogr., 51, 117–138,](#)  
3 [doi:10.1016/j.dsr2.2003.04.003, 2004.](#)

4 Arrigo, K. R. and Van Dijken, G. L.: Interannual variation in air-sea CO<sub>2</sub> flux in the Ross Sea,  
5 Antarctica: A model analysis, J. Geophys. Res., 112, 1–16, doi:10.1029/2006JC003492, 2007.

6 [Arrigo, K. R., van Dijken, G. L. and Bushinsky, S.: Primary production in the Southern Ocean,](#)  
7 [1997–2006, J. Geophys. Res., 113, C08004, doi:10.1029/2007JC004551, 2008.](#)

8 Arrigo, K. R., Robinson, D. H., Worthen, D. L., Dunbar, R. B., DiTullio, G. R., VanWoert, M.  
9 and Lizotte, M. P.: Phytoplankton community structure and the drawdown of nutrients and CO<sub>2</sub>  
10 in the Southern Ocean, Science, 283, 365–367, doi:10.1126/science.283.5400.365, 1999.

11 Arrigo, K. R., Worthen, D. L. and Robinson, D. H.: A coupled ocean-ecosystem model of the  
12 Ross Sea: 2. Iron regulation of phytoplankton taxonomic variability and primary production, J.  
13 Geophys. Res., 108, 3231, doi:10.1029/2001JC000856, 2003.

14 [Arrigo, K. R., van Dijken, G. L. and Bushinsky, S.: Primary production in the Southern Ocean,](#)  
15 [1997–2006, J. Geophys. Res., 113, C08004, doi:10.1029/2007JC004551, 2008.](#)

16 Bates, N. R., Hansell, D. A., Carlson, C. A. and Gordon, L. I.: Distribution of CO<sub>2</sub> species,  
17 estimates of net community production, and air-sea CO<sub>2</sub> exchange in the Ross Sea polynya, J.  
18 Geophys. Res., 103, 2883–2896, doi:10.1029/97jc02473, 1998.

19 Bates, N. R., Orchowska, M. I., Garley, R. and Mathis, J. T.: Summertime calcium carbonate  
20 undersaturation in shelf waters of the western Arctic Ocean – how biological processes  
21 exacerbate the impact of ocean acidification, Biogeosciences, 10, 5281–5309, doi:10.5194/bg-  
22 10-5281-2013, 2013.

23 Bednaršek, N., Tarling, G. a., Bakker, D. C. E., Fielding, S., Jones, E. M., Venables, H. J., Ward,  
24 P., Kuzirian, a., Lézé, B., Feely, R. a. and Murphy, E. J.: Extensive dissolution of live pteropods  
25 in the Southern Ocean, Nat. Geosci., 5, 881–885, doi:10.1038/ngeo1635, 2012.

26 [Bednaršek, N., Tarling, G. A., Bakker, D. C., Fielding, S. and Feely, R. A.: Dissolution](#)  
27 [dominating calcification process in polar pteropods close to the point of aragonite](#)  
28 [undersaturation, PLoS One, 9, e109183, doi:10.1371/journal.pone.0109183, 2014.](#)

1 Bresnahan, P. J., Martz, T. R., Takeshita, Y., Johnson, K. S. and Lashomb, M.: Best practices for  
2 autonomous measurement of seawater pH with the Honeywell Durafet, *Methods Oceanogr.*, 9,  
3 1–33, doi:10.1016/j.mio.2014.08.003, 2014.

4 Brewer, P. G. and Goldman, J. C.: Alkalinity changes generated by phytoplankton growth,  
5 *Limnol. Oceanogr.*, 21, 108–117, doi:10.4319/lo.1976.21.1.0108, 1976.

6 ~~[Burling, R. W.: Hydrology of circumpolar waters south of New Zealand, Zealand Department of](#)~~  
7 ~~[Scientific and Industrial Research Bulletin, 143, 66, 1961.](#)~~

8 ~~[Byrne, M., Ho, M. a., Koleits, L., Price, C., King, C. K., Virtue, P., Tilbrook, B. and Lamare, M.:](#)~~  
9 ~~[Vulnerability of the calcifying larval stage of the Antarctic sea urchin \*Sterechinus neumayeri\* to](#)~~  
10 ~~[near-future ocean acidification and warming, \*Glob. Chang. Biol.\*, 19, 2264–2275,](#)~~  
11 ~~[doi:10.1111/gcb.12190, 2013.](#)~~

12 Caldeira, K. and Wickett, M. E.: Oceanography: anthropogenic carbon and ocean pH., *Nature*,  
13 425, 365, doi:10.1038/425365a, 2003.

14 Chierici, M. and Fransson, A.: Calcium carbonate saturation in the surface water of the Arctic  
15 Ocean: undersaturation in freshwater influenced shelves, *Biogeosciences*, 6, 2421–2431,  
16 doi:10.5194/bg-6-2421-2009, 2009.

17 Collier, R., Dymond, J., Honjo, S., Manganini, S., Francois, R. and Dunbar, R.: The vertical flux  
18 of biogenic and lithogenic material in the Ross Sea: Moored sediment trap observations 1996–  
19 1998, *Deep. Res. Part II Top. Stud. Oceanogr.*, 47, 3491–3520, doi:10.1016/S0967-  
20 0645(00)00076-X, 2000.

21 ~~[Comeau, S., Gorsky, G., Alliouane, S., Gattuso, J.-P. and 10.1594/PANGAEA.733905: Larvae](#)~~  
22 ~~[of the pteropod \*Cavolinia inflexa\* exposed to aragonite undersaturation are viable but shell-less,](#)~~  
23 ~~[Mar. Biol., 157, 2341–2345, doi:10.1007/s00227-010-1493-6, 2010.](#)~~

24 ~~[Cummings, V., Hewitt, J., Van Rooyen, A., Currie, K., Beard, S., Thrush, S., Norkko, J., Barr,](#)~~  
25 ~~[N., Heath, P., Halliday, N. J., Sedcole, R., Gomez, A., McGraw, C. and Metcalf, V.: Ocean](#)~~  
26 ~~[acidification at high latitudes: potential effects on functioning of the Antarctic bivalve \*Laternula\*](#)~~  
27 ~~[elliptica, \*PLoS ONE\*, 6, e16069, doi:10.1371/journal.pone.0016069, 2011.](#)~~

28 Dickson, A. G.: The carbon dioxide system in seawater: equilibrium chemistry and  
29 measurements, in: *Guide to Best Practices in Ocean Acidification Research and Data Reporting*,

1 edited by: Riebesell, U., Fabry, V. J., Hansson, L., and Gattuso, J.-P., Luxembourg, Office for  
2 Official Publications of the European Communities, 17–40, 2010.

3 Dickson, A. G., and Millero, F. J.: A comparison of the equilibrium constants for the dissociation  
4 of carbonic acid in seawater media, *Deep Sea Res. Part A. Oceanogr. Res. Pap.*, 34, 1733–1743,  
5 doi:10.1016/0198-0149(87)90021-5, 1987.

6 Dickson, A. G., Afghan, J. D. and Anderson, G. C.: Reference materials for oceanic CO<sub>2</sub>  
7 analysis: a method for the certification of total alkalinity, *Mar. Chem.*, 80, 185–197,  
8 doi:10.1016/S0304-4203(02)00133-0, 2003.

9 Dickson, A. G., Sabine, C. L. and Christian, J. R.: Guide to best practices for ocean CO<sub>2</sub>  
10 measurements, *PICES Spec. Publ.*, 3, p191, doi:10.1159/000331784, 2007.

11 Dieckmann, G. S., Nehrke, G., Papadimitriou, S., Göttlicher, J., Steininger, R., Kennedy, H.,  
12 Wolf-Gladrow, D. and Thomas, D. N.: Calcium carbonate as ikaite crystals in Antarctic sea ice,  
13 *Geophys. Res. Lett.*, 35, 35–37, doi:10.1029/2008GL033540, 2008.

14 ~~Dong, S., Sprintall, J. and Gille, S. T.: Location of the Antarctic Polar Front from AMSR-E~~  
15 ~~Satellite Sea Surface Temperature Measurements, *J. Phys. Oceanogr.*, 36, 2075–2089,~~  
16 ~~doi:10.1175/JPO2973.1, 2006.~~

17 Dinniman, M. S., Klinck, J. M. and Smith, W. O.: A model study of Circumpolar Deep Water on  
18 the West Antarctic Peninsula and Ross Sea continental shelves, *Deep Sea Res. Part II Top. Stud.*  
19 *Oceanogr.*, 58, 1508–1523, doi:10.1016/j.dsr2.2010.11.013, 2011.

20 Ericson, J. A., Ho, M. A., Miskelly, A., King, C. K., Virtue, P., Tilbrook, B. and Byrne, M.:  
21 Combined effects of two ocean change stressors, warming and acidification, on fertilization and  
22 early development of the Antarctic echinoid *Sterechinus neumayeri*, *Polar Biol.*, 35, 1027–1034,  
23 doi:10.1007/s00300-011-1150-7, 2012.

24 Feely, R., Doney, S. and Cooley, S.: Ocean Acidification: Present Conditions and Future  
25 Changes in a High-CO<sub>2</sub> World, *Oceanography*, 22, 36–47, doi:10.5670/oceanog.2009.95, 2009.

26 Feng, Y., Hare, C. E., Rose, J. M., Handy, S. M., DiTullio, G. R., Lee, P. A., Smith, W. O.,  
27 Peloquin, J., Tozzi, S., Sun, J., Zhang, Y., Dunbar, R. B., Long, M. C., Sohst, B., Lohan, M. and  
28 Hutchins, D. A.: Interactive effects of iron, irradiance and CO<sub>2</sub> on Ross Sea phytoplankton,  
29 *Deep. Res. Part I Oceanogr. Res. Pap.*, 57, 368–383, doi:10.1016/j.dsr.2009.10.013, 2010.



1 Foster, B. A. and Montgomery, J. C.: Planktivory in benthic nototheniid fish in McMurdo Sound,  
2 Antarctica, *Environ. Biol. Fishes*, 36, 313–318, doi:10.1007/BF00001727, 1993.

3 Fransson, A., Chierici, M., Yager, P. L. and Smith, W. O.: Antarctic sea ice carbon dioxide  
4 system and controls, *J. Geophys. Res.*, 116, C12035, doi:10.1029/2010JC006844, 2011.

5 [Gannefors, C., Boer, M., Kattner, G., Graeve, M., Eiane, K., Gulliksen, B., Hop, H. and Falk-](#)  
6 [Petersen, S.: The Arctic sea butterfly \*Limacina helicina\*: lipids and life strategy, \*Mar. Biol.\*, 147,](#)  
7 [169–177, doi:10.1007/s00227-004-1544-y, 2005.](#)

8 [Gibson, J. A. . E. and Trull, T. W.: Annual cycle of fCO<sub>2</sub> under sea-ice and in open water in](#)  
9 [Prydz Bay, East Antarctica, \*Mar. Chem.\*, 66, 187–200, doi:10.1016/S0304-4203\(99\)00040-7,](#)  
10 [1999.](#)

11 [Gonzalez-Bernat, M. J., Lamare, M. and Barker, M.: Effects of reduced seawater pH on](#)  
12 [fertilisation, embryogenesis and larval development in the Antarctic seastar \*Odontaster validus\*,](#)  
13 [\*Polar Biol.\*, 36, 235–247, doi:10.1007/s00300-012-1255-7, 2013.](#)

14 Gordon, L. I., Codispoti, L. A., Jennings J.C., J., Millero, F. J., Morrison, J. M. and Sweeney, C.:  
15 Seasonal evolution of hydrographic properties in the Ross Sea, Antarctica, 1996-1997, *Deep-*  
16 *Res. Part II Top. Stud. Oceanogr.*, 47, 3095–3117, doi:10.1016/S0967-0645(00)00060-6, 2000.

17 [Hauck, J., Hoppema, M., Bellerby, R. G. J., Völker, C. and Wolf-Gladrow, D.: Data-based](#)  
18 [estimation of anthropogenic carbon and acidification in the Weddell Sea on a decadal timescale,](#)  
19 [\*J. Geophys. Res. Ocean.\*, 115, 1–14, doi:10.1029/2009JC005479, 2010.](#)

20 Hauck, J., Arrigo, K. R., Hoppema, M., Van Dijken, G. L., Völker, C. and Wolf-Gladrow, D. A.:  
21 Insignificant buffering capacity of Antarctic shelf carbonates, *Global Biogeochem. Cycles*, 27,  
22 11–20, doi:10.1029/2011GB004211, 2013.

23 Hauri, C., Gruber, N., Vogt, M., Doney, S. C., Feely, R. A., Lachkar, Z., Leinweber, A.,  
24 McDonnell, A. M. P. and Munnich, M.: Spatiotemporal variability and long-term trends of ocean  
25 acidification in the California Current System, *Biogeosciences*, 10, 193–216, doi:10.5194/bg-10-  
26 193-2013, 2013.

27 [Hofmann, G., Kelley, A. L., Shaw, E. C., Martz, T. R. and Hofmann, G. E.: Near shore Antarctic](#)  
28 [pH variability has implications for the design of ocean acidification experiments, \*Sci. Rep.\*, 5,](#)  
29 [9638, doi:10.1038/srep09638, 2015.](#)

1 [Hauri, C., Doney, S. C., Takahashi, T., Erickson, M., Jiang, G. and Ducklow, H. W.: Two](#)  
2 [decades of inorganic carbon dynamics along the Western Antarctic Peninsula, Biogeosciences](#)  
3 [Discuss., 12, 6929–6969, doi:10.5194/bgd-12-6929-2015, 2015.](#)

4 Hopkins, T. L.: Midwater food web in McMurdo Sound, Ross Sea, Antarctica, *Mar. Biol.*, 96,  
5 93–106, doi:10.1007/BF00394842, 1987.

6 Hunt, B. P. V, Pakhomov, E. A., Hosie, G. W., Siegel, V., Ward, P. and Bernard, K.: Pteropods  
7 in Southern Ocean ecosystems, *Prog. Oceanogr.*, 78, 193–221,  
8 doi:10.1016/j.pocean.2008.06.001, 2008.

9 IPCC AR5 WG1 (2013), Climate Change 2013: The Physical Science Basis. Contribution of  
10 Working Group I to the Fifth Assessment Report of the Intergovernmental Panel on Climate  
11 Change Rep., 1535 pp, Cambridge, United Kingdom and New York, NY, USA.

12 Jacobs, S. S.: On the nature and significance of the Antarctic Slope Front, *Mar. Chem.*, 35, 9–24,  
13 doi:10.1016/S0304-4203(09)90005-6, 1991.

14 Jacobs, S. S. and Giulivi, C. F.: Large multidecadal salinity trends near the Pacific-Antarctic  
15 continental margin, *J. Clim.*, 23, 4508–4524, doi:10.1175/2010JCLI3284.1, 2010.

16 Jacobs, S. S., Fairbanks, R. G., Horibe, Y.: Origin and evolution of water masses near the  
17 Antarctic continental margin: evidence from H<sub>2</sub><sup>18</sup>O/H<sub>2</sub><sup>16</sup>O ratios in seawater, in: *Oceanography*  
18 *of the Antarctic Continental Shelf*, Antarctic Research Series, 43, edited by: Jacobs, S. S.,  
19 American Geophysical Union, Washington, D.C, 59–85, 1985.

20 [Kapsenberg, L., Kelley, A. L., Shaw, E. C., Martz, T. R. and Hofmann, G. E.: Near-shore](#)  
21 [Antarctic pH variability has implications for the design of ocean acidification experiments, Sci.](#)  
22 [Rep., 5, 9638, doi:10.1038/srep09638, 2015.](#)

23 Kawaguchi, S., Ishida, A., King, R., Raymond, B., Waller, N., Constable, A., Nicol, S., Wakita,  
24 M. and Ishimatsu, A.: Risk maps for Antarctic krill under projected Southern Ocean  
25 acidification, *Nat. Clim. Chang.*, 3, 843–847, doi:10.1038/nclimate1937, 2013.

26 [Knap, A., Michaels A., Close A., Ducklow, H. and A. Dickson: Protocols for the Joint Global](#)  
27 [Ocean Flux Study \( JGOFS \) Core Measurements, JGOFS Rep., 19, 1–170, 1996.](#)

1 [Kohut, J., Hunter, E. and Huber, B.: Small-scale variability of the cross-shelf flow over the outer](#)  
2 [shelf of the Ross Sea. \*J. Geophys. Res. Ocean.\*, 118, 1863–1876. doi:10.1002/jgrc.20090, 2013.](#)

3 La Mesa, M., Vacchi, M. and Zunini Sertorio, T.: Feeding plasticity of *Trematomus newnesi*  
4 (Pisces, Nototheniidae) in Terra Nova Bay, Ross Sea, in relation to environmental conditions,  
5 *Polar Biol.*, 23, 38–45, doi:10.1007/s003000050006, 2000.

6 La Mesa, M., Eastman, J. T. and Vacchi, M.: The role of notothenioid fish in the food web of the  
7 Ross Sea shelf waters: A review, *Polar Biol.*, 27, 321–338, doi:10.1007/s00300-004-0599-z,  
8 2004.

9 Lee, K., Millero, F. J., Byrne, R. H., Feely, R. A. and Wanninkhof, R.: The recommended  
10 dissociation constants for carbonic acid in seawater, *Geophys. Res. Lett.*, 27, 229,  
11 doi:10.1029/1999GL002345, 2000.

12 Lenton, A., Codron, F., Bopp, L., Metzl, N., Cadule, P., Tagliabue, A. and Le Sommer, J.:  
13 Stratospheric ozone depletion reduces ocean carbon uptake and enhances ocean acidification,  
14 *Geophys. Res. Lett.*, 36, L12606, doi:10.1029/2009GL038227, 2009.

15 Lewis, E. and Wallace, D. W. R.: Program Developed for CO<sub>2</sub> System Calculations  
16 ORNL/CDIAC-105, Carbon Dioxide Information Analysis Centre, Oak Ridge National  
17 Laboratory, US Department of Energy, Tennessee, 1998.

18 Long, M. C., Dunbar, R. B., Tortell, P. D., Smith, W. O., Mucciarone, D. a. and Ditullio, G. R.:  
19 Vertical structure, seasonal drawdown, and net community production in the Ross Sea,  
20 Antarctica, *J. Geophys. Res. Ocean.*, 116, 1–19, doi:10.1029/2009JC005954, 2011.

21 Manno, C., Tirelli, V., Accornero, A. and Fonda Umani, S.: Importance of the contribution of  
22 limacina helicina faecal pellets to the carbon pump in terra nova bay (Antarctica), *J. Plankton*  
23 *Res.*, 32, 145–152, doi:10.1093/plankt/fbp108, 2010.

24 Matson, P. G., Washburn, L., Martz, T. R. and Hofmann, G. E.: Abiotic versus Biotic Drivers of  
25 Ocean pH Variation under Fast Sea Ice in McMurdo Sound, Antarctica, 9, e107239,  
26 doi:10.1371/journal.pone.0107239, 2014.

27 Mattsdotter Björk, M., Fransson, A., Torstensson, A. and Chierici, M.: Ocean acidification state  
28 in western Antarctic surface waters: Controls and interannual variability, *Biogeosciences*, 11,  
29 57–73, doi:10.5194/bg-11-57-2014, 2014.

1 [McClintock, J. B., Angus, R. a., Mcdonald, M. R., Amsler, C. D., Catledge, S. a. and Vohra, Y.](#)  
2 [K.: Rapid dissolution of shells of weakly calcified antarctic benthic macroorganisms indicates](#)  
3 [high vulnerability to ocean acidification. \*Antarct. Sci.\*, 21, 449–456,](#)  
4 [doi:10.1017/S0954102009990198, 2009.](#)

5 McClintock, J. B., Amsler, M. O., Angus, R. A., Challenger, R. C., Schram, J. B., Amsler, C. D.,  
6 Mah, C. L., Cuce, J. and Baker, B. J.: The Mg-Calcite Composition of Antarctic Echinoderms:  
7 Important Implications for Predicting the Impacts of Ocean Acidification, *J. Geol.*, 119, 457–  
8 466, doi:10.1086/660890, 2011.

9 McNeil, B. I. and Matear, R. J.: Southern Ocean acidification: a tipping point at 450-ppm  
10 atmospheric CO<sub>2</sub>, *Proc. Natl. Acad. Sci. U. S. A.*, 105, 18860–18864,  
11 doi:10.1073/pnas.0806318105, 2008.

12 McNeil, B. I., Metzl, N., Key, R. M., Matear, R. J. and Corbiere, A.: An empirical estimate of  
13 the Southern Ocean air-sea CO<sub>2</sub> flux, *Global Biogeochem. Cycles*, 21, GB3011,  
14 doi:10.1029/2007GB002991, 2007.

15 McNeil, B. I., Tagliabue, A. and Sweeney, C.: A multi-decadal delay in the onset of corrosive  
16 acidified waters in the Ross Sea of Antarctica due to strong air-sea CO<sub>2</sub> disequilibrium, *Geophys.*  
17 *Res. Lett.*, 37, 1–5, doi:10.1029/2010GL044597, 2010.

18 McNeil, B. I., Sweeney, C. and Gibson, J. A. E.: Short Note: Natural seasonal variability of  
19 aragonite saturation state within two Antarctic coastal ocean sites, *Antarct. Sci.*, 23, 411–412,  
20 doi:10.1017/S0954102011000204, 2011.

21 Mehrback, C., Culberson, C. H., Hawley, J. E. and Pytkowicz, R. M.: Measurement of the  
22 apparent dissociation constants of carbonic acid in seawater at atmospheric pressure, *Limnol.*  
23 *Oceanogr.*, 18, 897–907, doi:10.4319/lo.1973.18.6.0897, 1973.

24 Metzl, N., Brunet, C., Jabaud-Jan, A., Poisson, A. and Schauer, B.: Summer and winter air-sea  
25 CO<sub>2</sub> fluxes in the Southern Ocean, *Deep. Res. Part I Oceanogr. Res. Pap.*, 53, 1548–1563,  
26 doi:10.1016/j.dsr.2006.07.006, 2006.

27 [Millero, F. J., Lee, K. and Roche, M.: Distribution of alkalinity in the surface waters of the major](#)  
28 [oceans, in \*Marine Chemistry\*, 60, 111–130, 1998.](#)

1 Millero, F. J., Pierrot, D., Lee, K., Wanninkhof, R., Feely, R., Sabine, C. L., Key, R. M. and  
2 Takahashi, T.: Dissociation constants for carbonic acid determined from field measurements,  
3 Deep. Res. Part I Oceanogr. Res. Pap., 49, 1705–1723, doi:10.1016/S0967-0637(02)00093-6,  
4 2002.

5 Moy, A. D., Howard, W. R., Bray, S. G. and Trull, T. W.: Reduced calcification in modern  
6 Southern Ocean planktonic foraminifera, Nat. Geosci., 2, 276–280, doi:10.1038/ngeo460, 2009.

7 Mucci, A.: The solubility of calcite and aragonite in seawater at various salinities, temperatures,  
8 and one atmosphere total pressure., Am. J. Sci., 283, 780–799, doi:10.2475/ajs.283.7.780, 1983.

9 Orr, J. C., Fabry, V. J., Aumont, O., Bopp, L., Doney, S. C., Feely, R. A., Gnanadesikan, A.,  
10 Gruber, N., Ishida, A., Joos, F., Key, R. M., Lindsay, K., Maier-Reimer, E., Matear, R., Monfray,  
11 P., Mouchet, A., Najjar, R. G., Plattner, G.-K., Rodgers, K. B., Sabine, C. L., Sarmiento, J. L.,  
12 Schlitzer, R., Slater, R. D., Totterdell, I. J., Weirig, M.-F., Yamanaka, Y. and Yool, A.:  
13 Anthropogenic ocean acidification over the twenty-first century and its impact on calcifying  
14 organisms., Nature, 437, 681–686, doi:10.1038/nature04095, 2005.

15 Orsi, A. H. and Wiederwohl, C. L.: A recount of Ross Sea waters, Deep Sea Res. Part II Top.  
16 Stud. Oceanogr., 56, 778–795, doi:10.1016/j.dsr2.2008.10.033, 2009.

17 [Orsi, A. H., Whitworth, T. and Nowlin, W. D.: On the meridional extent and fronts of the](#)  
18 [Antarctic Circumpolar Current, Deep Sea Res. Part I Oceanogr. Res. Pap., 42, 641–673,](#)  
19 [doi:10.1016/0967-0637\(95\)00021-W, 1995.](#)

20 Petty, a. a., Holland, P. R. and Feltham, D. L.: Sea ice and the ocean mixed layer over the  
21 Antarctic shelf seas, Cryosphere, 8, 761–783, doi:10.5194/tc-8-761-2014, 2014.

22 Reuer, M. K., Barnett, B. A., Bender, M. L., Falkowski, P. G. and Hendricks, M. B.: New  
23 estimates of Southern Ocean biological production rates from O<sub>2</sub>/Ar ratios and the triple isotope  
24 composition of O<sub>2</sub>, Deep. Res. Part I Oceanogr. Res. Pap., 54, 951–974,  
25 doi:10.1016/j.dsr.2007.02.007, 2007.

26 [Riebesell, U., Zondervan, I., Rost, B., Tortell, P. D., Zeebe, R. E. and Morel, F. M.: Reduced](#)  
27 [calcification of marine plankton in response to increased atmospheric CO<sub>2</sub>, Nature, 407, 364–7,](#)  
28 [doi:10.1038/35030078, 2000.](#)

1 Rintoul, S., Hughes, C. and Olbers, D.: The Antarctic Circumpolar Current System BT - Ocean  
2 Circulation and Climate, in: Ocean Circulation and Climate, 271–301, 2001.

3 [Rivaró, P., Messa, R., Ianni, C., Magi, E. and Budillon, G.: Distribution of total alkalinity and  
4 pH in the Ross Sea \(Antarctica\) waters during austral summer 2008, \*Polar Res.\*, 33, 269,  
5 \[doi:10.3402/polar.v33.20403\]\(#\), 2014.](#)

6 Robbins, L. L., Wynn, J. G., Lisle, J. T., Yates, K. K., Knorr, P. O., Byrne, R. H., Liu, X.,  
7 Patsavas, M. C., Azetsu-Scott, K. and Takahashi, T.: Baseline monitoring of the western Arctic  
8 Ocean estimates 20% of Canadian basin surface waters are undersaturated with respect to  
9 aragonite., *PLoS One*, 8, e73796, [doi:10.1371/journal.pone.0073796](#), 2013.

10 [Rodén, N. P., Shadwick, E. H., Tilbrook, B. and Trull, T. W.: Annual cycle of carbonate  
11 chemistry and decadal change in coastal Prydz Bay, East Antarctica, \*Mar. Chem.\*, 155, 135–147,  
12 \[doi:10.1016/j.marchem.2013.06.006\]\(#\), 2013.](#)

13 Rubin, S. I.: Carbon and nutrient cycling in the upper water column across the Polar Frontal  
14 Zone and Antarctic Circumpolar Current along 170°W, *Global Biogeochem. Cycles*, 17, 1087,  
15 [doi:10.1029/2002GB001900](#), 2003.

16 Rubin, S. I., Takahashi, T., Chipman, D. W. and Goddard, J. G.: Primary productivity and  
17 nutrient utilization ratios in the Pacific sector of the Southern Ocean based on seasonal changes  
18 in seawater chemistry, *Deep. Res. Part I Oceanogr. Res. Pap.*, 45, 1211–1234,  
19 [doi:10.1016/S0967-0637\(98\)00021-1](#), 1998.

20 Saenz, B. T. and Arrigo, K. R.: Annual primary production in Antarctic sea ice during 2005-  
21 2006 from a sea ice state estimate, *J. Geophys. Res. Ocean.*, 119, 3645–3678,  
22 [doi:10.1002/2013JC009677](#), 2014.

23 [Sandrini, S., Ait-Ameur, N., Rivaró, P., Massolo, S., Touratier, F., Tositti, L. and Goyet, C.:  
24 Anthropogenic carbon distribution in the Ross Sea, Antarctica, \*Antarct. Sci.\*, 19, 395–407,  
25 \[doi:10.1017/S0954102007000405\]\(#\), 2007.](#)

26 [Schram, J. B., Schoenrock, K. M., McClintock, J. B., Amsler, C. D. and Angus, R. a.: Multi-  
27 frequency observations of seawater carbonate chemistry on the central coast of the western  
28 Antarctic Peninsula, \*Polar Res.\*, 1, 1–49, 2015.](#)

1 Seibel, B. A. and Dierssen, H. M.: Cascading Trophic Impacts of Reduced Biomass in the Ross  
2 Sea, Antarctica: Just the Tip of the Iceberg?, *Biol. Bull.*, 205, 93–97, 2003.

3 Sewell, M. A. and Hofmann, G. E.: Antarctic echinoids and climate change: A major impact on  
4 the brooding forms, *Glob. Chang. Biol.*, 17, 734–744, doi:10.1111/j.1365-2486.2010.02288.x,  
5 2011.

6 [Shadwick, E. H., Rintoul, S. R., Tilbrook, B., Williams, G. D., Young, N., Fraser, a. D.,  
7 Marchant, H., Smith, J. and Tamura, T.: Glacier tongue calving reduced dense water formation  
8 and enhanced carbon uptake, \*Geophys. Res. Lett.\*, 40, 904–909, doi:10.1002/grl.50178, 2013.](#)

9 Shadwick, E. H., Tilbrook, B. and Williams, G. D.: Carbonate chemistry in the Mertz Polynya  
10 (East Antarctica): Biological and physical modification of dense water outflows and the export  
11 of anthropogenic CO<sub>2</sub>, *J. Geophys. Res. Ocean.*, 119, 1–14, doi:10.1002/2013JC009286, 2014.

12 Smith, W. O. and Gordon, L. I.: Hyperproductivity of the Ross Sea (Antarctica) polynya during  
13 austral spring, *Geophys. Res. Lett.*, 24, 233, doi:10.1029/96GL03926, 1997.

14 Smith, W., Sedwick, P., Arrigo, K., Ainley, D. and Orsi, A.: The Ross Sea in a Sea of Change,  
15 *Oceanography*, 25, 90–103, doi:http://dx.doi.org/10.5670/oceanog.2012.80, 2012.

16 [Sokolov, S. and Rintoul, S. R.: Circumpolar structure and distribution of the antarctic  
17 circumpolar current fronts: 1. Mean circumpolar paths, \*J. Geophys. Res. Ocean.\*, 114, 1–19,  
18 doi:10.1029/2008JC005108, 2009.](#)

19 Spreen, G., Kaleschke, L. and Heygster, G.: Sea ice remote sensing using AMSR-E 89-GHz  
20 channels, *J. Geophys. Res. Ocean.*, 113, C02S03, doi:10.1029/2005JC003384, 2008.

21 [Stumpp, M., Hu, M. Y., Melzner, F., Gutowska, M. A., Dorey, N., Himmerkus, N., Holtmann,  
22 W. C., Dupont, S. T., Thorndyke, M. C. and Bleich, M.: Acidified seawater impacts sea urchin  
23 larvae pH regulatory systems relevant for calcification., \*Proc. Natl. Acad. Sci. U. S. A.\*, 109,  
24 18192–7, doi:10.1073/pnas.1209174109, 2012.](#)

25 [Suckling, C. C., Clark, M. S., Richard, J., Morley, S. a., Thorne, M. a. S., Harper, E. M. and  
26 Peck, L. S.: Adult acclimation to combined temperature and pH stressors significantly enhances  
27 reproductive outcomes compared to short-term exposures, \*J. Anim. Ecol.\*, 84, 773–784,  
28 doi:10.1111/1365-2656.12316, 2015.](#)

1 Sweeney, C.: The Annual Cycle of Surface Water CO<sub>2</sub> and O<sub>2</sub> in the Ross Sea : A model for Gas  
2 Exchange on the Continental Shelves of Antarctica, in: Biogeochemistry of the Ross Sea, 295–  
3 310. 2003.

4 Sweeney, C., Hansell, D. A., Carlson, C. A., Codispoti, L. A., Gordon, L. I., Marra, J., Millero,  
5 F. J., Smith, W. O. and Takahashi, T.: Biogeochemical regimes, net community production and  
6 carbon export in the Ross Sea, Antarctica, Deep. Res. Part II Top. Stud. Oceanogr., 47, 3369–  
7 3394, doi:10.1016/S0967-0645(00)00072-2, 2000a.

8 Sweeney, C., Smith, W. O., Hales, B., Bidigare, R. R., Carlson, C. A., Codispoti, L. A., Gordon,  
9 L. I., Hansell, D. A., Millero, F. J., Park, M. O. and Takahashi, T.: Nutrient and carbon removal  
10 ratios and fluxes in the Ross Sea, Antarctica, Deep. Res. Part II Top. Stud. Oceanogr., 47, 3395–  
11 3421, doi:10.1016/S0967-0645(00)00073-4, 2000b.

12 Swift, J .H., Orsi, A. H.: Sixty-four days of hydrography and storms: RVIB Nathaniel B.  
13 Palmer’s 2011 SO4P Cruise, Oceanography, 25, 54–55, doi:10.5670/oceanog.2012.74, 2012.

14 Tagliabue, A. and Arrigo, K. R.: Iron in the Ross Sea: 1. Impact on CO<sub>2</sub> fluxes via variation in  
15 phytoplankton functional group and non-Redfield stoichiometry, J. Geophys. Res. C Ocean.,  
16 110, 1–15, doi:10.1029/2004JC002531, 2005.

17 Takahashi, T., Sutherland, S. C., Wanninkhof, R., Sweeney, C., Feely, R. A., Chipman, D. W.,  
18 Hales, B., Friederich, G., Chavez, F., Sabine, C., Watson, A., Bakker, D. C. E., Schuster, U.,  
19 Metzl, N., Yoshikawa-Inoue, H., Ishii, M., Midorikawa, T., Nojiri, Y., Körtzinger, A., Steinhoff,  
20 T., Hoppema, M., Olafsson, J., Arnarson, T. S., Tilbrook, B., Johannessen, T., Olsen, A.,  
21 Bellerby, R., Wong, C. S., Delille, B., Bates, N. R. and de Baar, H. J. W.: Climatological mean  
22 and decadal change in surface ocean pCO<sub>2</sub>, and net sea-air CO<sub>2</sub> flux over the global oceans,  
23 Deep. Res. Part II Top. Stud. Oceanogr., 56, 554–577, doi:10.1016/j.dsr2.2008.12.009, 2009.

24 Tortell, P. D., Payne, C. D., Li, Y., Trimborn, S., Rost, B., Smith, W. O., Riesselman, C.,  
25 Dunbar, R. B., Sedwick, P. and DiTullio, G. R.: CO<sub>2</sub> sensitivity of Southern Ocean  
26 phytoplankton, Geophys. Res. Lett., 35, L04605, doi:10.1029/2007GL032583, 2008.

27 van Heuven, S., Pierrot, D., Rae, J. W. B., Lewis, E., and Wallace, D. W. R.: MATLAB program  
28 developed for CO<sub>2</sub> system calculations, ORNL/CDIAC-105b, Carbon Dioxide Information



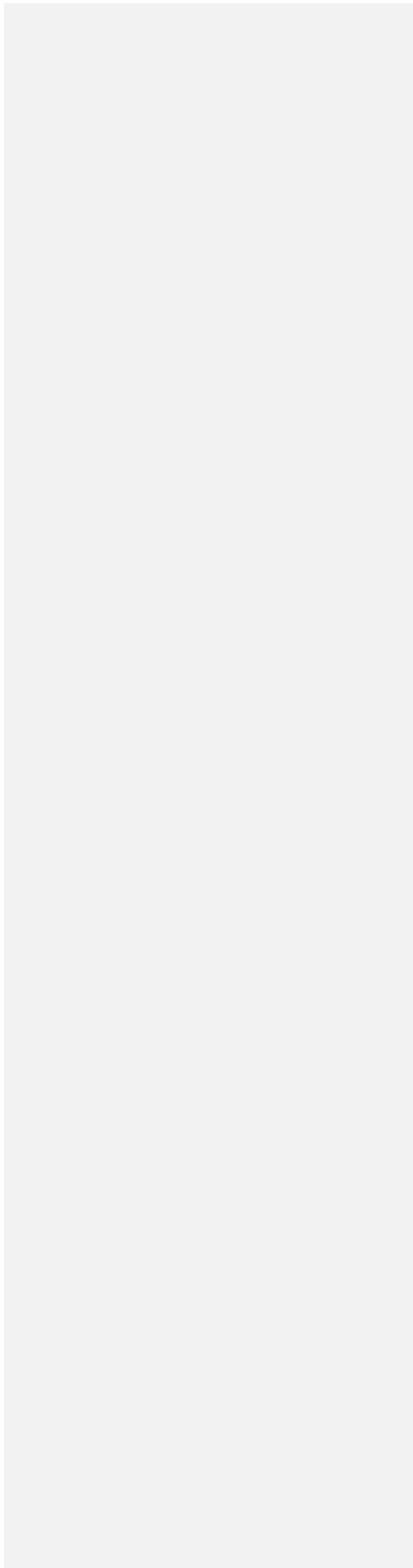
1 Analysis Center, Oak Ridge National Laboratory, US Department of Energy, Oak Ridge,  
2 Tennessee, doi:10.3334/CDIAC/otg.CO2SYS MATLAB v1.1, 2011.

3 [Weeber, a., Swart, S. and Monteiro, P. M. S.: Seasonality of sea ice controls interannual](#)  
4 [variability of summertime  \$\Omega\$  at the ice shelf in the](#)  
5 [Eastern Weddell Sea – an ocean acidification sensitivity study, Biogeosciences](#)  
6 [Discuss., 12, 1653–1687, doi:10.5194/bgd-12-1653-2015, 2015.](#)

7 Yamamoto-Kawai, M., McLaughlin, F. A., Carmack, E. C., Nishino, S. and Shimada, K.:  
8 Aragonite undersaturation in the Arctic Ocean: effects of ocean acidification and sea ice melt,  
9 Science, 326, 1098–1100, doi:10.1126/science.1174190, 2009.

10 [Yu, P. C., Sewell, M. a., Matson, P. G., Rivest, E. B., Kapsenberg, L. and Hofmann, G. E.:](#)  
11 [Growth attenuation with developmental schedule progression in embryos and early larvae of](#)  
12 [Sterechnus neumayeri raised under elevated CO<sub>2</sub>, PLoS One, 8, e52448,](#)  
13 [doi:10.1371/journal.pone.0052448, 2013.](#)

14  
15  
16  
17  
18  
19  
20  
21  
22  
23  
24  
25  
26  
27



1 **Table 1.** Mean values for sDIC concentrations below 200 m

Data source	Early Spring	Spring	Summer	Autumn
Sweeney et al. (2000)	2226 ± 3	2233 ± 3	2237 ± 3	2233 ± 5
Long et al. (2011 )		2224 ± 5	2225 ± 4	
This paper				2220 ± 5

1 **Table 2.** Water properties of CDW from McNeil et al. (2010) and CLIVAR

Data source	Salinity	DIC ( $\mu\text{mol kg}^{-1}$ )	TA ( $\mu\text{mol kg}^{-1}$ )	PO <sub>4</sub> ( $\mu\text{mol kg}^{-1}$ )	SiO <sub>4</sub> ( $\mu\text{mol kg}^{-1}$ )	$\Omega_{\text{Ar}}$
McNeil et al. (2010)	34.70 $\pm$ 0.02	2255 $\pm$ 1	2330	2.22 $\pm$ 0.01	93.5 $\pm$ 1.2	1.01
CLIVAR	34.71 $\pm$ 0.02	2257 $\pm$ 3	2348 $\pm$ 4	2.21 $\pm$ 0.04	95.6 $\pm$ 6.0	1.18

1 ~~Fig. 1. Cruise track (black line) from NBP 13-02. Stations used in this study (red circles) from~~  
2 ~~(a) TRACERS (NBP 13-02) and (b) CLIVAR (NBP 11-02). Blue line is the 1000 m isobath.~~

3  
4 **Fig. 21.** Maps of (a) 6.25 km gridded sea ice concentration on 1 Dec 2012 from the University of  
5 Bremen, <http://www.iup.uni-bremen.de:8084/amsr2/#Antarctic> (Spreen et al., 2008), (b) sea  
6 surface salinity from NBP 13-02, (c) satellite chlorophyll concentration on Feb 2013 from the 9  
7 km level 3 Aqua MODIS product, <http://oceancolor.gsfc.nasa.gov/cgi/13>, (d) sTA from NBP 13-  
8 02, (e) pCO<sub>2</sub> from NBP 13-02 (f) aragonite saturation state ( $\Omega_{Ar}$ ) from NBP 13-02.

9  
10 ~~Fig. 12. Cruise track (black line) from NBP 13-02. Stations used in this study (red circles) from~~  
11 ~~(a) TRACERS (NBP 13-02) and (b) CLIVAR (NBP 11-02). Blue line is the 1000 m isobath.~~

12  
13 **Fig. 3.** Contributions of sDIC, sTA, temperature, salinity, and ~~pTA-PALK~~ to changes in the  
14 aragonite saturation state ( $\Omega_{Ar}$ ) of surface waters from the winter to early autumn. Error bars  
15 represent  $\pm 1$  S.D.

16  
17 **Fig. 4.** Surface water properties from a Southern Ocean transect, 20 March – 2 April 2013: (a)  
18 aragonite saturation state ( $\Omega_{Ar}$ ), (b) SST, (c) pCO<sub>2</sub>, and (d) particulate organic carbon. The  
19 locations of the Subantarctic Front (SAF), the Polar Front (PF), and the southern Antarctic  
20 Circumpolar Current Front (SACCF) from Sokolov and Rintoul (2009) ~~Polar Front (PF) and~~  
21 ~~Sub-Antarctic Front (SAF)~~ are indicated (grey dashed-lines).

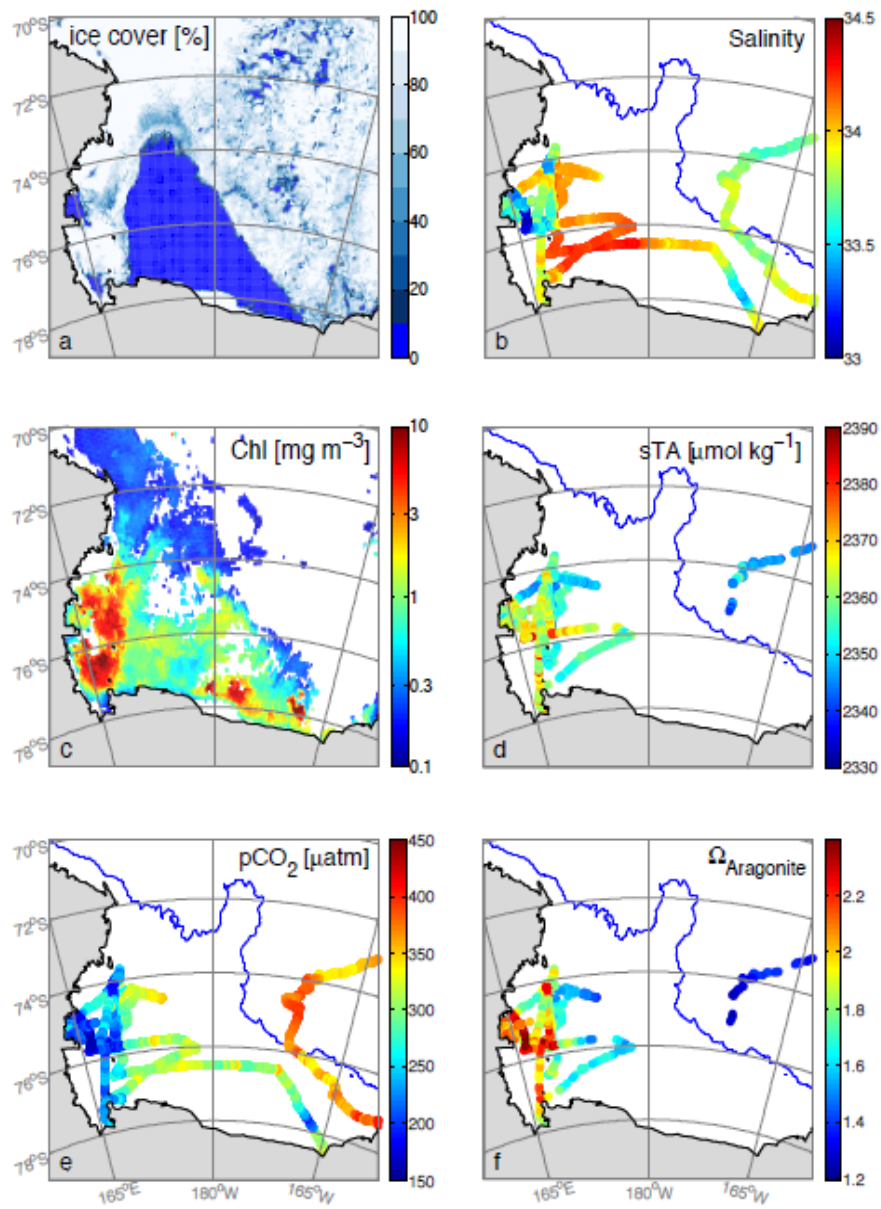
22  
23 **Fig. 5.** From surface water measurements along a Southern Ocean transect (a) contributions of  
24 changing sDIC (red), sTA (blue), temperature (green), and salinity (magenta) to changing  
25 aragonite saturation state (black,  $\Omega_{Ar}$ ) relative to the start of the transect and (b) TA to DIC  
26 ratios. The locations of the Subantarctic Front (SAF), the Polar Front (PF), and the southern  
27 Antarctic Circumpolar Current Front (SACCF) from Sokolov and Rintoul (2009) ~~Polar Front~~  
28 ~~(PF) and Sub-Antarctic Front (SAF)~~ are indicated (grey dashed-lines).  
29

1 **Fig. 6.** Measured surface water salinity normalized (a) DIC calculated from pCO<sub>2</sub>, TA,  
2 temperature, and salinity and (b) TA. The locations of the Subantarctic Front (SAF), the Polar  
3 Front (PF), and the southern Antarctic Circumpolar Current Front (SACCF) from Sokolov and  
4 Rintoul (2009) Polar Front (PF) and Sub-Antarctic Front (SAF) are indicated (grey dashed-lines).  
5

6 **Fig. 7.** Estimating winter surface aragonite saturation states ( $\Omega_{Ar}$ ): (a) map of surface pCO<sub>2</sub>  
7 measurements from the LDEO pCO<sub>2</sub> database (<http://www.ldeo.columbia.edu/res/pi/CO2>) used  
8 in this study from November 1994 (blue), 1997 (red), 2005 (green), and 2006 (black). Blue line  
9 is the 1000 m isobath. ~~(b) Linear regression between TA and salinity with surface data from~~  
10 ~~February–March 2013 (blue, this study), November–December 1994 (green, Bates et al.,~~  
11 ~~1998), December–January 1995/1996 (red, Bates et al., 1998), and April 1997 (magenta,~~  
12 ~~Sweeney et al., 2000). TA has been corrected to a nitrate concentration of 29  $\mu\text{mol kg}^{-1}$  to~~  
13 ~~account for the effects of nitrate drawdown on TA (Brewer and Goldman, 1976).~~ (eb) aragonite  
14 saturation state ( $\Omega_{Ar}$ ) of surface waters from November calculated from pCO<sub>2</sub>, salinity derived  
15 TA, temperature, and salinity (d) ~~profiles of aragonite saturation state ( $\Omega_{Ar}$ ) from off the Ross~~  
16 ~~Shelf (see Fig. 1) from NBP 11-02 calculated from TA, DIC, temperature, and salinity at surface~~  
17 ~~pressures.~~

18  
19  
20  
21  
22  
23  
24  
25  
26  
27  
28  
29  
30  
31

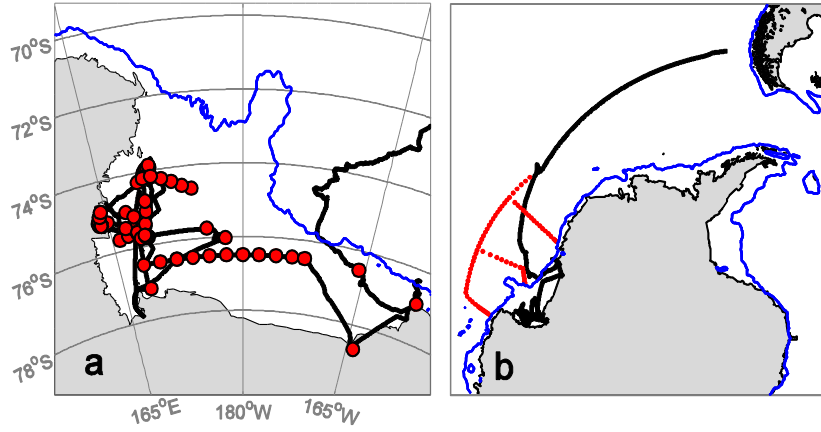
1 [Fig. 1](#)



2

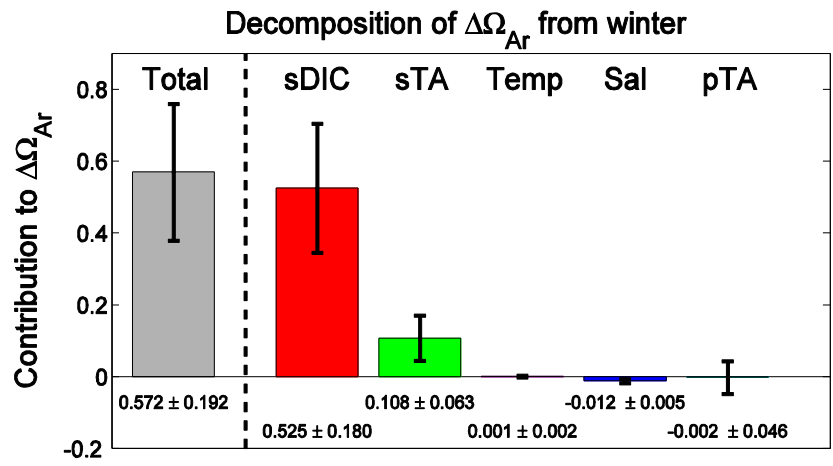
1 Fig. 2

Formatted: Font: (Default) Times New Roman, Not Bold



- 2
- 3
- 4
- 5
- 6
- 7
- 8
- 9
- 10
- 11
- 12
- 13
- 14
- 15
- 16

1 **Fig. 3**



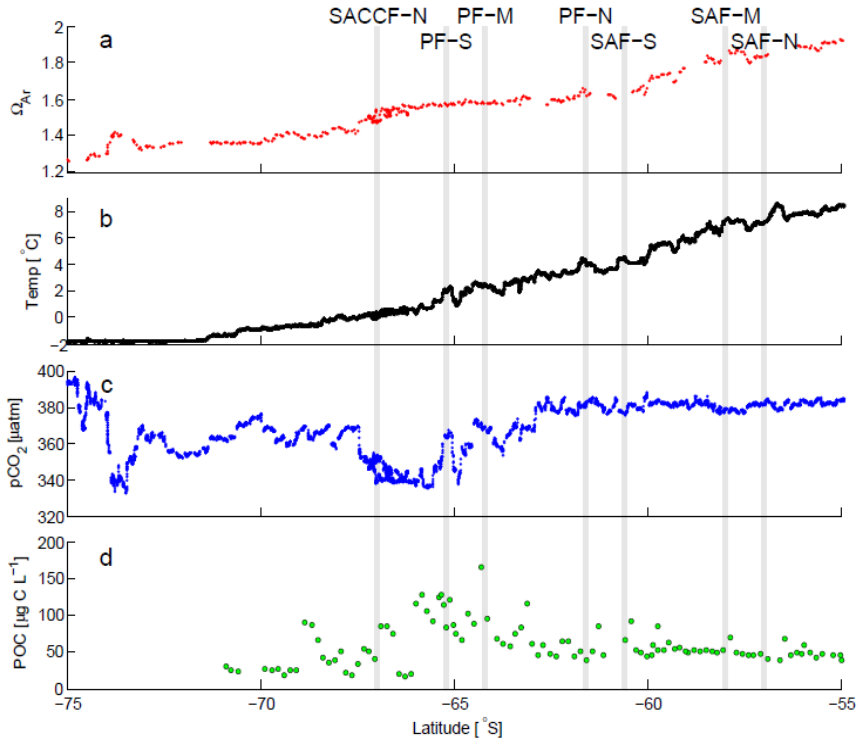
**Formatted:** Font: (Default) Times New Roman

**Formatted:** Font: (Default) Times New Roman, Not Bold

2  
3  
4  
5  
6  
7  
8  
9  
10  
11  
12  
13  
14  
15



1 [Fig. 4](#)



2

3

4

5

6

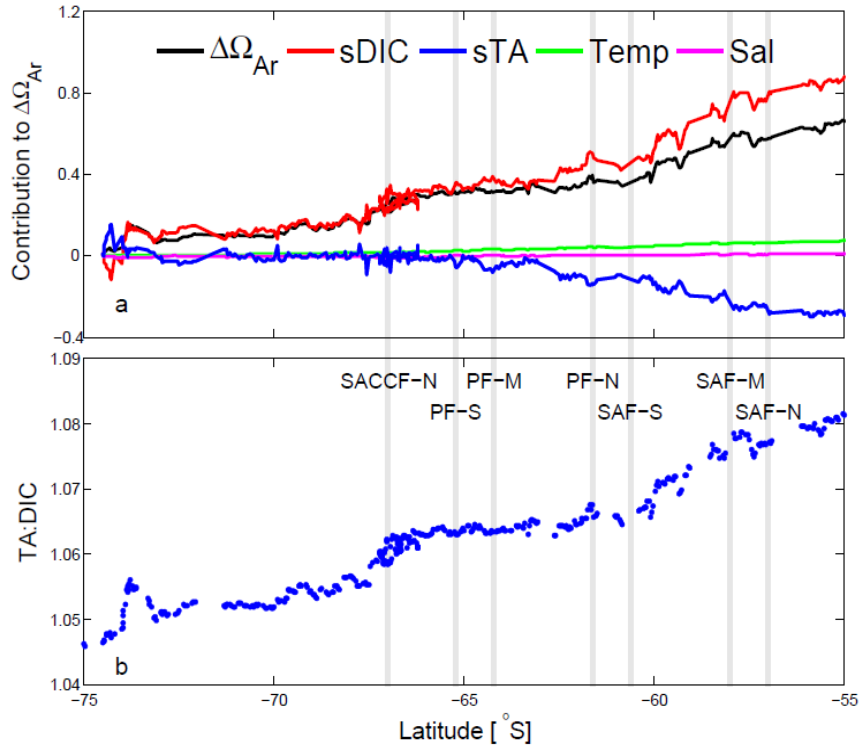
7

8

9

10

1 [Fig. 5](#)



2

3

4

5

6

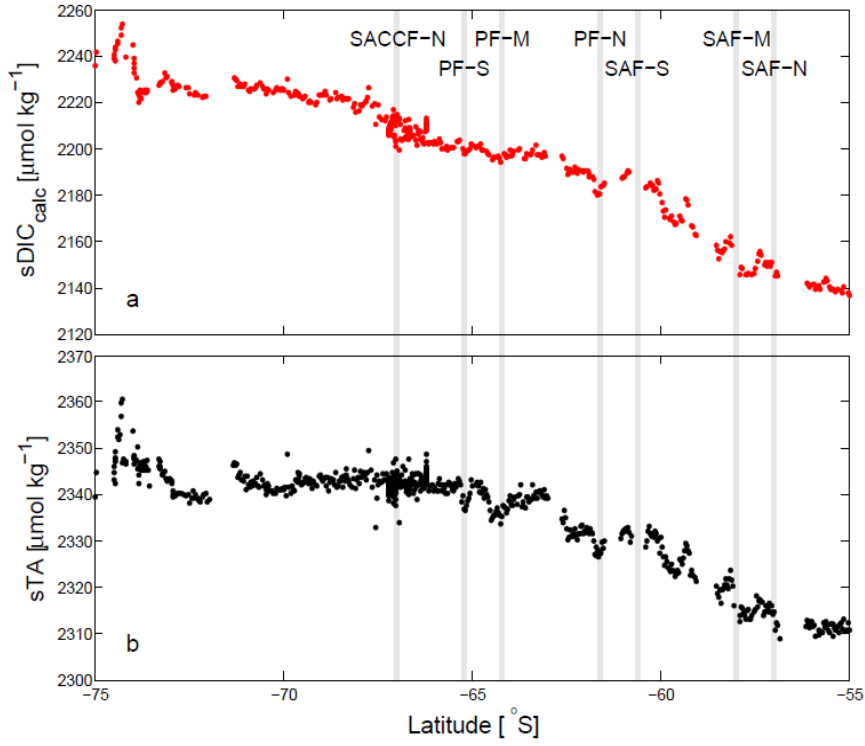
7

8

9

10

1 [Fig. 6](#)



2

3

4

5

6

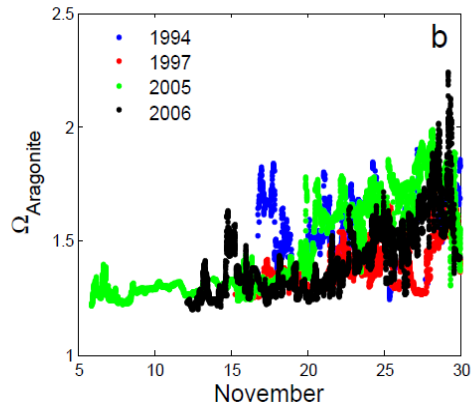
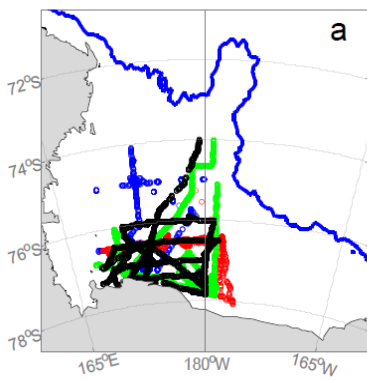
7

8

9

10

1 Fig. 7



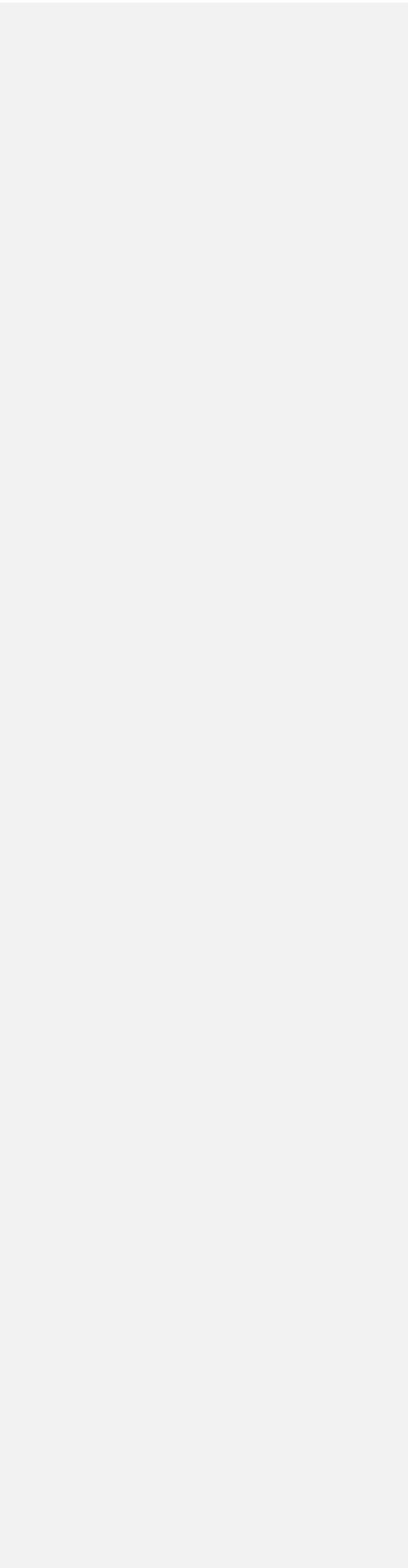
2  
3  
4  
5  
6  
7  
8  
9  
10  
11  
12  
13  
14  
15  
16

1 **Appendix**

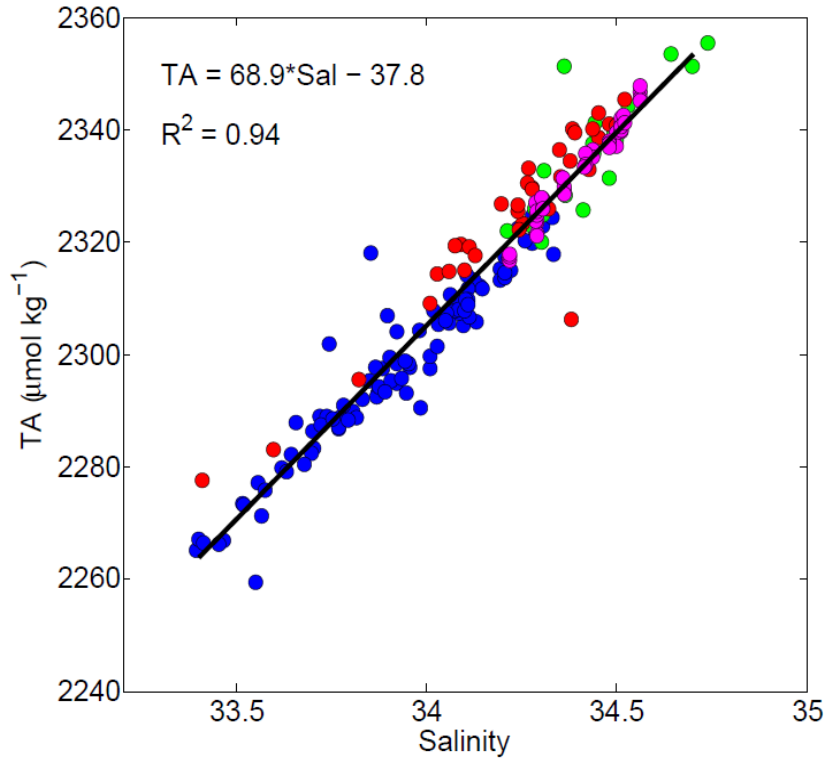
2  
3 **Fig. A1.** ~~(b)~~ Linear regression between TA and salinity with surface data from February –  
4 March 2013 (blue, this study), November – December 1994 (green, Bates et al., 1998),  
5 December – January 1995/1996 (red, Bates et al., 1998), and April 1997 (magenta, Sweeney et  
6 al., 2000a). TA has been corrected to a nitrate concentration of 29  $\mu\text{mol kg}^{-1}$  to account for the  
7 effects of nitrate drawdown on TA (Brewer and Goldman, 1976).

8  
9 **Fig. A2.** ~~(d)~~ Profiles of aragonite saturation state ( $\Omega_{Ar}$ ) from off the Ross Shelf (see Fig. 42b)  
10 from the CLIVAR program (NBP 11-02) calculated from TA, DIC, temperature, and salinity at  
11 surface pressures.

12  
13  
14  
15  
16  
17  
18  
19  
20  
21  
22  
23  
24  
25  
26  
27  
28  
29  
30  
31

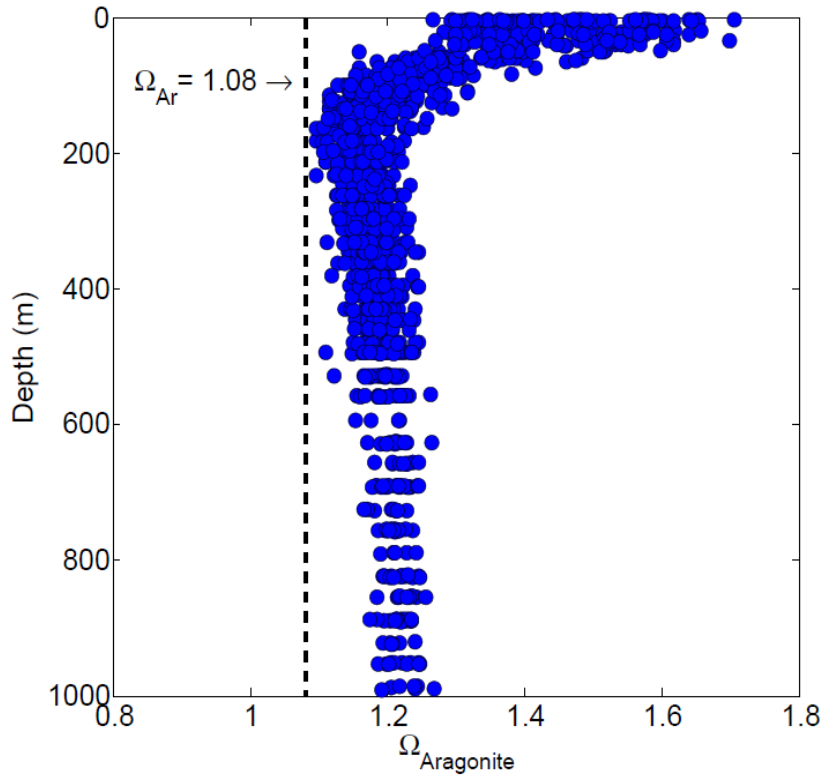


1 [Fig. A1](#)



2  
3  
4  
5  
6  
7  
8  
9  
10  
11  
12  
13

1 [Fig. A2](#)



2  
3  
4  
5  
6

---